Review

Mariano A. Kappes*

Localized corrosion and stress corrosion cracking of stainless steels in halides other than chlorides solutions: a review

https://doi.org/10.1515/corrrev-2019-0061
Received July 5, 2019; accepted October 20, 2019; previously published online December 20, 2019

Abstract: Fluorides, bromides, and iodides, despite being less common than chlorides, are present in various environments of industrial relevance. Stainless steels suffer pitting corrosion in solutions of all halides except fluorides, which can be understood considering that fluoride is the anion of a weak acid. The aggressiveness of the rest of the halides for pitting corrosion is on the order $Cl^- > Br^- > I^-$ for stainless steels with Mo content below 3 wt.%. Mo is not as effective in inhibiting Br^- pitting corrosion as it is for inhibiting Cl^- pitting corrosion. Most of those observations were rationalized based on the effect of anions on pit growth kinetics. Sensitized austenitic stainless steel suffers stress corrosion cracking (SCC) in solutions of all halides, albeit chlorides seem to be the most aggressive. Fluoride SCC is relevant for SCC under insulation of stainless steels, and standards and regulations developed to mitigate this problem consider this ion as aggressive as chloride. For the solubilized stainless steels, aggressiveness toward SCC is in the order $Cl^- > Br^-$. The SCC of solubilized stainless steels was not observed in solutions of F^- and I^-, and the possible reasons for this fact are discussed.

Keywords: fluorides; halides; pitting; stainless steels; stress corrosion cracking.

1 Introduction

Chlorides are present in a wide variety of industrial environments (Kolotyrkin, 1963; Brown, 1977), including fossil and nuclear power plants, food, paper, pulp, and chemical industry and petroleum refineries. Therefore, pitting, crevice corrosion, and stress corrosion cracking (SCC) of stainless steels were extensively studied in chloride solutions (Brown, 1977; Cragnolino et al., 1981; Cragnolino & Macdonald, 1982; Haruyama, 1982; Sedriks, 1996; Frankel, 1998; Szklarska-Smialowska, 2005). Given those considerations, this review will be focused on SCC and pitting corrosion of stainless steels in solutions of halides other than chlorides, in particular, at a temperature below 100°C.

The SCC of stainless steel was observed in solutions of all halide ions. The SCC in F^- and I^- solutions was only reported for alloys in the sensitized condition (Table 1). Sensitization occurs by exposure of stainless steels to elevated temperatures during welding, heat treatment, or service conditions, causing chromium carbide precipitation at grain boundaries and depletion in chromium close to grain boundaries, thus, favoring intergranular (IG) attack and intergranular stress corrosion cracking (IGSCC). A remarkable observation is that IGSCC was observed in laboratory tests even when F^- concentration in the solutions was as low as 1 ppm (Ward et al., 1969; Theus & Cels, 1974). Pitting corrosion of stainless steels, on the other hand, occurs in solutions of all halides except F^- (Table 1). Moreover, F^- can act as an inhibitor of pitting and crevice corrosion in chloride solutions (Yamazaki, 1994, 1996), and this was explained based on the fact that it is the anion of a weak acid.

2 Abundance of halogens in nature

Fluorine (F), chlorine (Cl), bromine (Br), iodine (I), and astatine (At) are the elements of the halogen family that occur naturally on Earth. Astatine is the scarcest of the naturally occurring elements (Greenwood & Earnshaw, 1997), and it is radioactive with a half-life of 8.1 h for its most stable isotope (Lide, 2005). Therefore, At is not

***Corresponding author: Mariano A. Kappes,** Instituto Sabato (UNSAM/CNEA), CONICET, Comisión Nacional de Energía Atómica, Av. Gral. Paz 1499, San Martín, Buenos Aires 1650, Argentina, e-mail: marianokappes@gmail.com. https://orcid.org/0000-0002-5708-5565

further discussed in this review. The rest of the elements in the halogen family achieve a stable configuration by forming diatomic molecules: F_2 and Cl_2 are gases, Br_2 is a liquid, and I_2 is solid at ambient temperature and pressure. However, due to their reactivity, halogens occur in nature as halides (X^-), and iodine also occurs as iodate (IO_3^-) (Greenwood & Earnshaw, 1997). The abundance of elements in crustal rocks decreases with an increase in the atomic mass of the halogen element (Greenwood & Earnshaw, 1997). While fluoride is more abundant than chloride in crustal rocks, fluoride is mainly present in minerals that are scarcely soluble in water, like fluorite or fluorspar (CaF_2), cryolite (Na_3AlF_6), and fluorapatite ($CaF_2 \cdot 3Ca_3(PO_4)_2$), whereas chloride is mainly present in water-soluble rock salt (NaCl) (Chambers & Holliday, 1975; Greenwood & Earnshaw, 1997). Chloride is the dominant anion in ocean water, where its concentration is 1.9 wt.% (Greenwood & Earnshaw, 1997), about 15,000 times higher than F^- (Warner, 1971) and 290 times higher than Br^- (Stine, 1929). Iodine is less abundant than lighter halogens both in the earth's crust and in ocean water. Iodine is a micronutrient necessary for various organisms (Ito, 1988). In seawater, it can be present as I^- and IO_3^-, with total inorganic iodine in ocean water at around 0.05 ppm (Ito, 1988). The concentration of halide ions in seawater is summarized in Table 1. Chloride dominates in aerosols in the atmosphere, and they can contact metals by direct deposition or after dissolution in rainwater. The main sources of chlorides in aerosols are the ocean, road deicing salts, or the products of the combustion of fossil fuels and residues (Willison et al., 1989).

3 Stability of halides in water

The stable oxidation number of fluorine and chlorine throughout the range of stability of water is –1 (Pourbaix, 1966). In dilute solutions of hydrofluoric acid (HF), F^- dominate at pH >3.17 (Mccoubrey, 1955), which is the pk_a of HF (Table 1). Below this pH, HF dominates (Pourbaix, 1966). In more concentrated solutions (greater than 3.8 g F/l), the bifluoride ion, HF_2^-, predominates in the pH region close to pk_a (Pourbaix, 1966). Hydrochloric acid, HCl, is a strong acid; hence, it is completely dissociated in water, and the stable form of chlorine in water solutions is as Cl^-. Bromine is stable as Br^- in almost the entire range of water stability, except for very low pH and oxidizing conditions, where it can react according to (Pourbaix, 1966):

$$2Br^-(ac) \rightarrow Br_2(l) + 2e^- \quad E_0 = 1.082\,V_{SHE} \tag{1}$$

Iodine has the lowest standard reduction potential of the halogen group ($E_0 = 0.62\ V_{SHE}$), and aqueous I^- solutions are thermodynamically unstable in the presence of dissolved oxygen, reacting to give IO_3^- (Pourbaix, 1966):

$$I^-(ac) + 3H_2O \rightarrow IO_3^-(ac) + 6H^+(ac) + 6e^- \quad E_0 = 1.085\,V_{SHE} \tag{2}$$

IO_3^- is the thermodynamically stable form of iodine in seawater, but I^- is produced by biologically mediated reduction of IO_3^- or under reducing conditions (Ito, 1988). In acid media, the intermediate formation of I_2 or I_3^- (triiodide) occurs according to (Pourbaix, 1966):

$$3I^-(ac) \rightarrow I_3^-(ac) + 2e^- \quad E_0 = 0.536\,V_{SHE} \tag{3}$$

Table 1: Selected properties of the halides and overview of observed modes of corrosion of stainless steel in halide solutions.

Halide ion, X^-	F^-	Cl^-	Br^-	I^-	References
Radius of X^- (nm)	0.133	0.181	0.196	0.219	Chambers & Holliday, 1975
ΔG_0^{hyd} (kJ/mol)	−472	−351	−326	−294	Macdonald & Lei, 2016
pKa of HX	3.17	−7	−9	−10	Mccoubrey, 1955; Greenwood & Earnshaw, 1997
Concentration in seawater (ppm)	1.3	19×10^3	65	0.05 (present as I^- and IO_3^-)	Stine, 1929; Warner, 1971; Ito, 1988; Greenwood & Earnshaw, 1997
Pitting of stainless steel in X^- solutions	No	Yes	Yes	Yes	Tzaneva et al., 2006; Macdonald & Lei 2016; Pahlavan et al., 2016
SCC of stainless steel in X^- solutions	Only in sensitized condition	Yes	Yes	Only in sensitized condition	Rhodes, 1969; Ward et al., 1969; Theus & Cels, 1974; Griess et al., 1985; Takemoto et al., 1985; Trabanelli et al., 1988; Zucchi et al., 1988; Itzhak & Elias, 1994; Itzhak et al., 1996; Whorlow & Hutto, 1997; Downs et al., 2007; Sridhar et al., 2017

$$2I_3^-(ac) \rightarrow 3I_2(ac) + 2e^- \quad E_0 = 0.789\,V_{SHE} \tag{4}$$

4 Presence of halides in industrial environments

4.1 Fluorides

In industrial applications of stainless steels, some relevant sources of F^- are thermal insulation (Takemoto et al., 1985; Whorlow et al., 1997) and electrode coatings and fluxes used during welding operation (Ward et al., 1969; Takemoto et al., 1985). Fluorinated hydrocarbons used in lubricants and gaskets can liberate F^- at the temperature of operation of pressurized or boiling water reactors (Brown, 1977). Fluorides are present in pickling solutions of stainless steels. Pickling is a surface process that removes metallic contamination, besides welding and heat treatment scales. This process is typically performed by immersion in nitric and hydrofluoric acid solutions, but it is explicitly not recommended for sensitized stainless steels by ASTM A380 (ASTM A380-17, 2017), due to possible intergranular attack and SCC even under ambient conditions (Berry et al., 1973). Fluoridation is the addition of F^- to a public water supply to prevent tooth decay, and it is targeted to maintain a concentration of about 1 ppm in water (Greenwood & Earnshaw, 1997). Cryolite is used in the electrolysis of alumina for metallic aluminum production (Greenwood & Earnshaw, 1997). Fluorine has a key role in the nuclear fuel cycle (Crouse, 2015), where it is used to produce gaseous UF_6 from which fissionable isotopes can be separated by different technologies.

4.2 Bromides

Industrial applications of bromine compounds used to be dominated by 1,2-dibromoethane or ethylene dibromide, a compound added to gasoline as a lead scavenger, until environmental legislation limited the use of lead-based anti-knock additives (Greenwood & Earnshaw, 1997; Thomas et al., 1997). Ethylene dibromide and methyl bromide have applications as pesticides as well (Greenwood & Earnshaw, 1997). Other major applications of bromine compounds are as flame retardants, in plastics, fibers, rugs, and carpets. Silver bromide, AgBr, is an active compound in photographic films. Some catalysts for chemical industries contain bromides, and this caused pitting of a type 316L stainless steel component handling organic acids (Ohtsu & Miyazawa, 2012). Bromides are present in high-density brine completion fluids, applied to deep oil and gas wells to balance the high pressure of the well and maintain the borehole stability (Liu et al., 2014). Those fluids typically contain bromides or chlorides of Ca, Zn, and Na (Sridhar et al., 2017). Calcium bromide is used for controlling mercury emissions of coal-fired power plants (Ladwig & Blythe, 2017). The salt decomposes in the furnace to yield bromine or hydrogen bromide, and they react with elemental mercury. Oxidized mercury compounds are then more easily captured in downstream wet scrubbers for flue gas desulfurization. However, bromides can cause localized corrosion problems of materials used for wet scrubbers (Ozturk & Grubb, 2012).

Concentrated LiBr brines have applications in absorption refrigeration systems (Itzhak & Elias, 1994; Srikhirin et al., 2001). The main advantage of those systems is that a compressor is not used. Water is used as the refrigerant, and when it evaporates at low pressure, heat is absorbed from the environment. This water vapor is absorbed by concentrated LiBr brines. The brine, now diluted, is heated in a generator. The brine becomes concentrated, and evaporated water from it is condensed in a heat exchanger. The condensed water and concentrated brine are now ready to start a new cycle. Stainless steels are frequently used in metallic parts of those systems, which motivated corrosion studies in concentrated (above 50%) LiBr brines at temperature in the range from 80°C to 160°C (Griess et al., 1985; Guiñon et al. 1994; Itzhak & Elias, 1994; Itzhak et al., 1996).

4.3 Iodides

Iodine solutions are commonly used in redox titrations. Iodine is scarcely soluble in water, but solubility increases in iodide solutions by the following complexation reaction (Harris, 2007):

$$I^-(ac) + I_2(ac) \rightarrow I_3^-(ac) \tag{5}$$

I_3^- solutions can be used to titrate solutions of reducing agents, using starch as an indicator. Oxidizing solutions are treated with I^- to produce an excess of I_3^-, which is then titrated with thiosulfate (Harris, 2007).

$$I_3^-(ac) + 2S_2O_3^{2-}(ac) \rightarrow 3I^-(ac) + S_4O_6^{2-}(ac) \tag{6}$$

Triiodide solutions have applications as antiseptic for cuts and wounds (Chambers & Holliday 1975). Stainless

steels 304L and 316L exhibit pitting in iodine solutions or solutions exposed to iodine vapor, as reported by Tsukaue et al. (1993, 1994a,b) at temperatures in the range from 50°C to 80°C. Triiodide is involved in the cathodic reaction (Eq. (3)). Iodides produced in this reaction favor the solubility of iodine so that the reactant of the cathodic reaction is regenerated by Eq. (5). This causes the accumulation of triiodide in stainless steels, resulting in stable pit growth (Tsukaue et al., 1994a,b). Iodine is a dangerous fission product that could be released in accidents of nuclear power plants (Wren et al., 1999). The amount of iodine released to the environment is monitored with sampling systems that have stainless steel lines that transport gases through filters and absorbers where the presence and concentration of radionuclides are analyzed (Evans & Nugraha, 2002). It was shown that with water vapor content above 75% and above 10^{-9} M I_2 in the gas, aqueous pitting corrosion by iodine is possible (Evans & Nugraha, 2002). Besides the integrity problem in the material of the sampling line, the amount of iodine transmitted through the line is reduced, causing errors in the monitoring process (Evans & Nugraha, 2002).

5 Pitting corrosion in halides other than chloride solutions

Pitting corrosion of stainless steels involves breakdown of the passive film, metastable pitting, and stable growth of pits (Frankel et al., 2017). Breakdown of the passive film was explained by halide adsorption and thinning of the passive film, halide penetration, and the film-breaking mechanism, as reviewed in-depthly elsewhere (Frankel, 1998; Szklarska-Smialowska, 2005; Soltis, 2015). Halide ions affect properties of the passive film, for example, XPS studies show that the thickness of the passive film of iron in buffer solution decreases as the concentration of Cl^-, Br^-, and I^- increases (Khalil et al., 1985), and Cl^- is the most aggressive for a given concentration. The point defect model was also applied to analyze passivity breakdown in solutions of the different halide ions (Macdonald & Lei, 2016). The model successfully predicts that the ability of halide ions to cause passivity breakdown is in the order $F^- \ll Cl^- > Br^- > I^-$. According to this model, passivity breakdown first requires absorption of the halide ion into the passive film. In short, halide ions absorb by occupying surface oxygen anion vacancies, and this process requires expansion of the oxygen vacancy to accommodate the halide ion with a larger diameter, dehydration of the halide ion, and insertion of the halide ion into the expanded oxygen vacancy. By considering the Gibbs free energy required for each of those processes, a minimum in breakdown potential was predicted for Cl^- solutions. The exceptionally high stability of hydrated F^- ions is elucidated in Table 1 by the Gibbs free energy values of halide anion hydration, ΔG_0^{hyd}, (Macdonald & Lei, 2016). The high energy required for F^- dehydration results in the absence of passivity breakdown in F^- solutions.

Despite those effects of halide ions on properties and breakdown of the passive film, it is known that breakdown events of the passive film can occur at a very high rate, as evidenced during metastable pitting at potentials below the stable pitting potential, E_{pit} (Frankel et al., 2017). Those frequent events of passive film breakdown and metastable growth are not a problem for structural integrity if repassivation of the passive film is rapid (Frankel et al., 2017). Furthermore, stainless steels for industrial applications usually have appreciable fractions of inclusions or second phase particles, which provide favorable sites for pit initiation and possibly sulfur-containing aggressive species to the local environment (Frankel, 1998). Therefore, the main attention is often targeted to understanding the conditions required for stable growth, or in other words, those that make a metastable pit grow stably (Frankel, 1998; Newman, 2001; Li et al., 2018). Like many other variables that affect pitting corrosion resistance (Newman, 2001), the aggressiveness of the different halide ions can be understood in terms of their effect on stable pit growth rather than on pit nucleation.

The aggressiveness of the different halide anions can be ranked by comparison of pitting potential (E_{pit}), the repassivation potential (E_{rp}) or the critical pitting temperature (CPT) at a given molar concentration of the anion, or by evaluating the minimum amount required for stable pit growth (Szklarska-Smialowska, 2005).

5.1 Fluoride solutions

Hydrofluoric acid is a weak acid, with a pK_a of 3.17 (Mccoubrey, 1955) (Table 1). The rest of the acids are strong, meaning that they completely dissociate in water. The localized acidification theory of pitting corrosion (Galvele, 1976) predicts that the anions of weak acids act as inhibitors. In accord with those considerations, pitting corrosion of stainless steels was not observed in fluoride solutions at room temperature (Streicher, 1956; Koch, 1993). Studied materials where this was verified include quenched and tempered martensitic 403 stainless steel (Pahlavan et al., 2016), supermartensitic 13 Cr stainless steel (Macdonald & Lei, 2016), sensitized 304 stainless steel (Zucchi et al., 1988),

17 wt.% Cr, 12 wt.% Mn and 0.61 wt.% N stainless steel, and 18 wt.% Cr with 9 wt.% Ni stainless steels (Tzaneva et al., 2006). The absence of pitting was confirmed by either observation of specimens after the test or absence of hysteresis in the return potential scanning curve.

While type 304 sensitized stainless steel suffer intergranular attack and SCC in the presence of F^- ions (Ward et al., 1969; Theus & Cels, 1974), breakdown of the passive layer was not observed in the absence of stress at room temperature (Trabanelli et al., 1988; Zucchi et al., 1988). The Cr content near the grain boundary of sensitized stainless steel is controlled by the bulk chemical composition of the stainless steel, time, and temperature in the carbide precipitation region, and grain size. For type 304 stainless steel, scanning transmission electron microscope (STEM) studies coupled with X-ray energy-dispersive spectroscopy (EDS) revealed that the Cr content near the grain boundary can decrease to 13 wt.% or less (Rao, 1979; Ford & Silverman, 1980; Thorvaldsson & Salwén, 1984). Despite this depletion in Cr at the grain boundary, as the potential was increased in the anodic direction, polarization curves of sensitized type 304 stainless steel in F^- solutions at room temperature exhibited a passive behavior, followed by a current increase in the potential range corresponding to oxygen evolution (Zucchi et al., 1988). No hysteresis was observed on the potential scan in the noble direction, confirming that localized corrosion did not occur even at the most positive potentials (Zucchi et al., 1988). In accord with those studies, anodic polarization in F^- solutions did not cause breakdown of the passive layer in martensitic stainless steels (Pahlavan et al. 2016), where the bulk Cr content was close to the Cr content near the grain boundary of sensitized 304 stainless steel.

Despite stable pitting is not observed in fluoride solutions, Macdonald and Lei (2016) reported metastable pitting for a 13 Cr martensitic stainless steel in 0.1 M NaF solution. The rate of metastable pitting events and the average current density increased in the order $F^- < I^- < Br^- < Cl^-$. The average current density of metastable pits in F^- solutions was one order of magnitude lower than in Cl^- solutions (Macdonald & Lei 2016). The low frequency of those events and their low current might explain why other authors working in similar systems reported the absence of metastable pitting in F^- solutions (Pahlavan et al., 2016).

5.2 Fluorides as inhibitors of Cl^- pitting and crevice corrosion

It was shown that F^- increases the pitting initiation (Yamazaki, 1994) and crevice corrosion initiation and repassivation (Yamazaki, 1996, 1997) potential of type 304 stainless steel in Cl^- solutions. This increase in the pitting potential when F^- is added to Cl^- solutions was also reported by Pahlavan et al. (2016) for type 403 martensitic stainless steel. Interestingly, when F^- was added to Cl^- solutions, the rate of nucleation of metastable pits increased (Pahlavan et al., 2016). Therefore, F^- appear to inhibit the stable growth of pits, and this was explained on the basis of Galvele's localized acidification theory (Galvele, 1976). The high pK_a of HF results in F^- bonding to H^+ at pit bottoms, therefore, inhibiting pit growth (Pahlavan et al., 2016).

5.3 Pitting corrosion in halides and strength of the hydrohalide acid

Stable pitting of stainless steels was observed in solutions of the rest of the halides. The strength of the acid increases from HCl to HI (Table 1) (Chambers & Holliday, 1975), but because they are all strong and completely dissociated in water, this difference in strength can only be observed in solvents more acidic than water, for example, acetic acid. In aqueous solution, this difference in strength is irrelevant because they are all leveled out to H_3O^+ (Chambers & Holliday, 1975), and in fact, the aggressiveness of the different anions for pitting corrosion of stainless steels and passive iron in aqueous solutions generally increases from $I^- < Br^- < Cl^-$ (Tousek, 1975; Janik-Czachor, 1979; Szklarska-Smialowska, 2005; Tzaneva et al., 2006; Pahlavan et al., 2016). A notable exception to this rule is observed in Mo alloyed stainless steels, where it was found that Br^- ions are more aggressive than Cl^- (Guo & Ives, 1990; Kaneko & Isaacs, 2002) above a certain content of Mo, as discussed in a subsequent section.

5.4 Effect of halide ion concentration on the pitting potential

Pitting potentials (E_{pit}) decrease with an increase in the concentration of the aggressive ion, $[X^-]$, according to (Galvele, 1976; Szklarska-Smialowska, 2005):

$$E_{pit} = a - B \log[X^-] \quad (7)$$

where a and B are constants. The B value is controlled by the charge of the aggressive anion and complexation reactions between metal cations and anions inside the pit (Nguyen et al., 2019). Without complexation, a B value of 59 mV is predicted for all halide ions at room

temperature (Galvele, 1976; Nguyen et al., 2019). For pure iron in borate buffer solutions containing Cl^-, Br^-, or I^-, Janik-Czachor (1979) reported a *B* value of 100 mV, irrespective of the nature of the halide ion. For pure iron, this is an unusually high value, considering other studies (Galvele, 1976; Nguyen et al., 2019) in Cl^- solutions, where it was reported to be close to 59 mV. On the other hand, for stainless steels that suffer pitting at room temperature, the reported B values in Cl^- solutions are close to 90 mV (Galvele, 1976; Laycock & Newman, 1997; Nguyen et al., 2019). The B value increases with the stability constant of the metal-chloride complex, and stainless steels contain chromium, which forms complexes more stable than iron (Nguyen et al., 2019). Measurements in martensitic stainless steels (Pahlavan et al., 2016) revealed that the B value for Cl^-, Br^-, and I^- was 130, 80, and 76 mV, respectively. For type 316 austenitic stainless steel, a slope of 91 mV was reported for Cl^- solutions and of 75 mV in Br^- solutions (Pahlavan et al., 2019a). In other words, an equal increase in halide ion concentration will cause a higher decrease in pitting potential for Cl^- than for the rest of the halides.

5.5 Adsorption of the halides and pitting corrosion

The halide ion radius and the strength of the adsorbed halide-metal bond increase with atomic mass (Table 1) (de Castro & Wilde, 1979; Szklarska-Smialowska, 2005) so that larger iodide ion adsorption is thermodynamically more favored than fluoride adsorption. Therefore, the anions that adsorb more strongly to the metal are less aggressive for pitting (Szklarska-Smialowska, 2005). A plausible explanation for this fact could be that adsorption of halide ions to the bare metal surface exposed to an acid solution can inhibit active dissolution of the metal, under certain conditions. Cl^-, Br^-, and I^- additions to a H_2SO_4 solution result in lower rates of active metal dissolution, as it is observed for mild steel (Jesionek & Szklarska-Smialowska, 1983), pure nickel (Abd El Rehim et al., 1986), and 18 Cr-8 Ni stainless steel (Asawa, 1971). An inhibiting effect on carbon steel corrosion is also observed when KF is added to 0.01 M H_2SO_4 solutions (Sekine et al., 1994), but this is probably related to a buffering effect of F^- ions.

The strength of adsorption of halides to active metal, the surface coverage of halides and the inhibition efficiency increase with increasing halide ion size (Jesionek & Szklarska-Smialowska, 1983; Abd El Rehim et al., 1986). However, this inhibiting effect of halides on active dissolution of metals in acid solutions is observed below a concentration that is specific for each halide ion and material (Asawa, 1971; Jesionek & Szklarska-Smialowska, 1983; Abd El Rehim et al., 1986) and around 10^{-2} M (Abd El Rehim et al., 1986). For Ni in sulfuric acid solutions (Abd El Rehim et al., 1986), when halide ions are present at a concentration above 10^{-2} M, they accelerate anodic dissolution and shift the active to passive transition to higher potential, and the aggressiveness increases in the order $I^- < Br^- < Cl^-$. A similar effect is observed in 18 Cr-8 Ni stainless steels in 4 N H_2SO_4 (Asawa, 1971), for concentrations of halide ions up to 1 M. At the bottom of a pit under sustained growth, the concentration of halide ions can be much higher, on the order of 8 M or more (Mankowski & Szklarska-Smialowska, 1975). The effect of halide ion on metal dissolution at those concentrations was studied with the artificial pit electrode, as will be discussed below.

Pitting corrosion studies with wire electrodes showed an "anomalous" higher aggressiveness of Br^- vs. Cl^- (Carroll & Lynskey, 1994), under a wide range of experimental variables. The pitting potential was lower in Br^- than in Cl^- solutions for types 316, 304L, and 302 stainless steel wires, measured in solutions of pH ranging from 3 to 9 and halide concentration ranging from 0.1 M to 1 M. This anomalous effect was associated to a refining effect of the wire-drawing process on inclusions like sulfides (Pistorius & Burstein, 1992), which act as favorable sites for pit initiation of stainless steels in Cl^- solutions (Szklarska-Smialowska, 2005). On the other hand, pitting potentials in bromide solutions were similar whether they were measured with wire electrodes or electrodes cut from bars, suggesting that pitting initiation in Br^- solutions relies more on the adsorption of Br^- ions than on interaction with inclusions. According to the authors (Carroll & Lynskey, 1994), Br^- has a greater tendency to adsorb on the metal surface than Cl^-, and this has a greater effect on pit initiation when there is a low population of sulfides. Measurements of pitting potential of 316L stainless steels electrodes cut from bars, with a regular population of sulfides, showed the higher aggressiveness of Cl^- vs. Br^- usually observed for low Mo stainless steels.

5.6 Pit growth in Cl^- vs. Br^- solutions

Pit growth can be studied independently of pit initiation with the "lead-in-pencil" or artificial pit electrode technique (Laycock & Newman, 1997; Kaneko & Isaacs, 2000; Ernst & Newman, 2008). A survey of the literature published up to date reveals that this technique was used to study pit growth kinetics in Br^- vs. Cl^- solutions (Kaneko & Isaacs, 2000; Pahlavan et al., 2019a,b), but no studies were reported in I^- solutions. In this technique, a wire of

the metal or alloy to be studied is embedded in epoxy, and after dissolving back the metal at an anodic potential, a one-dimensional artificial pit is eventually formed after the conglomeration of smaller pits (Laycock & Newman, 1997). The electrochemical potential is then scanned in the active direction, while the current is measured. Figure 1 shows the polarization curves of artificial pit electrodes obtained in Br^- vs. Cl^- solutions, for an 18 wt.% Cr-12 wt.% Ni austenitic stainless steel (Kaneko & Isaacs, 2000). Similar results were obtained by Pahlavan et al. (2019a) for a type 316 austenitic stainless steel. A region where current is independent of potential is observed in Figure 1. In this region, a salt film is precipitated on the metal surface, and the current density of the unidimensional pit is diffusion limited (i_{lim}) (Laycock & Newman, 1997):

$$i_{lim} = \frac{n F D C_{sat}}{x} \tag{8}$$

where n is the average charge of metal ions, F is Faraday's constant, D is the effective or average diffusion coefficient of metal cations, C_{sat} is the molar concentration of metal ions in the saturated halide salt solution, and x is the depth of the unidimensional pit. Notice that Eq. (8) is based on Fick's first law of diffusion and, therefore, is strictly valid during steady state. Because of metal dissolution, x increases with time. However, relative changes of x during the characteristic time of diffusion, x^2/D, are small enough for the approximation to be valid (Laycock & Newman, 1997). As a consequence, despite x increases as potential is scanned in the active direction, i_{lim} is independent of potential for scan rates in the range of 1 mV/s to 10 mV/s, typically used in this experiment (Laycock & Newman 1997; Li et al. 2019).

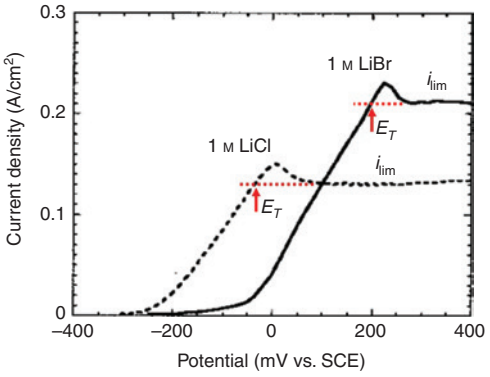

Figure 1: Anodic polarization curves of 18 wt.% Cr–12 wt.% Ni stainless steel, obtained for a 0.44-mm deep artificial pit electrode in 1 M LiCl and 1 M LiBr bulk solutions. The electrochemical potential was scanned at a rate of 5 mV/s in the active direction. E_T is the transition potential, where anodic dissolution shifts from diffusion control to activation/ohmic control. Adapted from Corrosion Science, 42(1), Kaneko and Isaacs, Pitting of stainless steel in bromide, chloride and bromide/chloride solutions, 67–78, Copyright (2000), with permission from Elsevier.

It is expected that the most prominent element in the alloy will precipitate first (Bocher et al., 2010). For stainless steel, ferrous halide should dominate in the salt film. However, how chromium, nickel, and the rest of the alloying and impurity elements affect the precipitation of iron halides is not known in depth. Kaneko and Isaacs (2000) argue that the concentration of saturated $FeBr_2$ should be similar to saturated $FeCl_2$ and around 5 M. In that case, the reason for the higher diffusion-limited current density reported in the literature (Kaneko & Isaacs, 2000; Pahlavan et al., 2019a) and schematized in Figure 1 resides in a higher diffusion coefficient of metallic cations in Br^- vs. Cl^- solutions, which is roughly estimated to be within a factor of 1.5. As potential is decreased, eventually, the salt film is dissolved, which is indicated by a small hump in the i vs. E curve (Ernst & Newman, 2008) (Figure 1). Current then decreases sharply with potential, due to ohmic drop and activation control.

The transition potential, E_T, is the minimum applied potential required for salt film precipitation at the pit bottom. From Figure 1, this potential can be estimated as the potential, where $E = i_{lim}$, on the left of the hump associated with salt film dissolution (Laycock & Newman, 1997; Ernst & Newman, 2008). The actual potential at the pit bottom might be lower due to an ohmic drop in potential, and it can be estimated by different procedures detailed in the literature (Gaudet et al., 1986; Laycock & Newman 1997; Li et al., 2019). An increase in E_T measured with pencil electrodes correlated with an increase in E_{pit} measured on flat electrodes, as the Br^-/Cl^- concentration ratio increased in solutions with a total halide concentration of 0.2 M (Pahlavan et al. 2019b). Kaneko and Isaacs (2000) reported similar results for 1 M Br^- and 1 M Cl^- solutions. According to Laycock and Newman (1997), stable pitting requires the precipitation of a salt film at the pit bottom, thus, explaining the correlation between E_T and E_{pit}. While a solution saturated in metallic cations is the most aggressive solution attainable at the pit bottom at a given temperature, recent studies confirm that stable pitting can be sustained in less concentrated solutions (Srinivasan & Kelly, 2017; Li et al., 2019). For example, according to Srinivasan and Kelly (2017), stable pitting of a 316L stainless steel at room temperature requires a concentration around 50% of the saturated solution at the pit bottom (Srinivasan & Kelly, 2017), otherwise the pit repassivates.

A deeper understanding of how measurements with the artificial pit electrode can explain E_{pit} differences in Br^- vs. Cl^- solutions can be achieved with a suitable model for pit growth (Li et al., 2018; Pahlavan et al., 2019b). During pitting corrosion, metallic cations are produced by anodic dissolution at the pit bottom and diffuse out of the pit down a concentration gradient. Mathematically, a stable growth of pits requires that (Li et al., 2018)

$$i_{diss,max} \geq i_{diff,crit} \tag{9}$$

where $i_{diss,max}$ is the maximum anodic dissolution current at the pit bottom for a given temperature, pit solution concentration, and potential, and $i_{diff,crit}$ is the critical current density for diffusion of metal cations out of the pit. In other words, the rate of production of metallic ions at the pit bottom must compensate its loss by diffusion out of the pit, otherwise, dilution and repassivation occur. The expression for $i_{diff,crit}$ for unidimensional pits is similar to Eq. (8), but C_{crit} is a fraction of C_{sat} (Li et al., 2018):

$$i_{diff,crit} = \frac{n F D C_{crit}}{x} \tag{10}$$

From artificial pit experiments and a diffusion model (Gaudet et al., 1986), Kaneko and Isaacs (2000) argue that to prevent pit repassivation, a higher concentration of metallic ions is required in Br^- vs. Cl^- solutions, i.e. C_{crit} in Br^- will be higher than C_{crit} in Cl^- in Eq. (10). As previously discussed, the diffusion coefficient of metallic cations is higher in Br^- vs. Cl^- solutions, according to experiments conducted by Kaneko and Isaacs (2000). Therefore, from Eqs. (9) and (10) and for a given pit depth x, pit stability in Br^- solutions requires a higher dissolution current $i_{diss,max}$ at the pit bottom. Finally, considering the curves presented in Figure 1, it is inferred that for a given current density, a higher potential is required to attain it in Br^- vs. Cl^- solutions. Notice that this analysis was made considering unidimensional pits, but it can be extended because similar expressions hold for hemispherical pits (Li et al., 2018). All those contributions explain the higher E_{pit} observed in Br^- vs. Cl^- solutions (Kaneko & Isaacs, 2000; Pahlavan et al., 2019a,b), confirming that the higher aggressiveness of Br^- vs. Cl^- ions can be explained on the basis of pit growth kinetics.

5.7 The Mo effect in Br^- vs. Cl^- solutions

Ferritic (Kaneko & Isaacs, 2002) and austenitic (Guo & Ives, 1990; Kaneko & Isaacs, 2002) stainless steels alloyed with Mo can be more susceptible to pitting in Br^- vs. Cl^- solutions. A higher pitting potential was measured in Br^- vs. Cl^- solutions when Mo content was low (Guo & Ives, 1990; Kaneko & Isaacs, 2002; Pahlavan et al., 2019a); however, Mo additions had a stronger inhibiting effect on the pitting potential in Cl^- than in Br^- solutions (Horvath & Uhlig, 1968). Hence, above a certain Mo content that depended on stainless steel microstructure (Kaneko & Isaacs, 2002), Br^- became more aggressive than Cl^-, causing stable pitting at lower potentials. Those results were in good correlation with anodic polarization curves measured with the artificial pit electrode (Kaneko & Isaacs, 2002). In Cl^- solutions, studies with the artificial pit electrode reveal that Mo increases pitting resistance by shifting the bare metal anodic dissolution curve to higher potentials (Laycock & Newman, 1997). This displacement of the anodic curve for a given increment of Mo is lower in Br^- solutions vs. Cl^- solutions (Kaneko & Isaacs, 2002). This lower effect of Mo in preventing Br^- pitting was attributed to the formation of soluble molybdenum complexes (Newman, 2001), a lower production of inhibiting polymolybdate species in bromide solutions (Domínguez-Aguilar & Newman, 2006), or to the fact that when Br^- displaces the anodic dissolution curve to a higher potential, as schematized in Figure 1, Mo dissolves more easily, and it is less effective as an inhibitor (Ernst & Newman, 2008).

For commercial steels, E_{pit} in Cl^- is lower than E_{pit} in Br^- for type 304 stainless steel (Ernst & Newman, 2008), type 301 stainless steel (0.19% Mo as impurity) (Guo & Ives, 1990), type 316 stainless steel (2.5% Mo) (Guo & Ives, 1990; Ernst & Newman, 2008; Pahlavan et al., 2019a), and type UNS S31260 (3% Mo) duplex stainless steel (Yamamoto & Hosoya, 1995). The reverse behavior is observed for type 904L (UNS N08904) with 4.5 wt.% Mo (Guo & Ives, 1990; Abd El Meguid, 1997) and for 6% Mo superaustenitic stainless steel (UNS S31254) (Guo & Ives, 1990). Some of those results are summarized in Figure 2 for measurements of E_{pit} near room temperature.

5.8 PRE_N and localized corrosion resistance in Br^- solutions

With the exception of Mo, how effective the different alloying elements are for preventing localized corrosion in Br^- and I^- solutions was not as deeply and systematically studied as in Cl^- solutions. For Cl^- solutions, the beneficial effect of Cr, Mo, W, and N on pitting and crevice corrosion resistance of stainless steels is often summarized with the

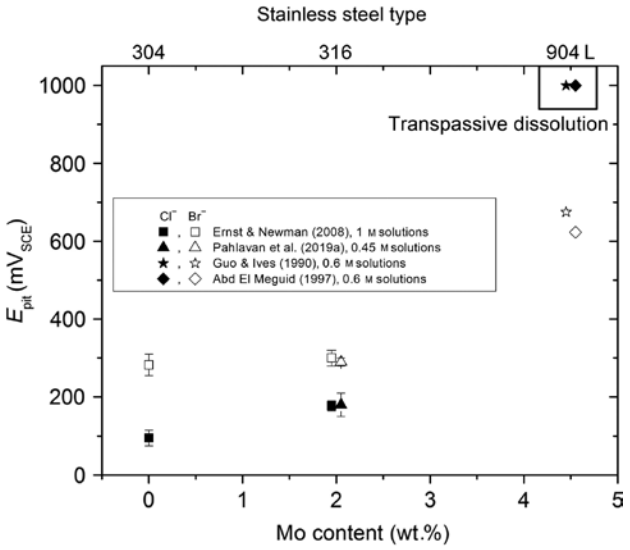

Figure 2: Effect of molybdenum content on the pitting potential, E_{pit}, in Cl^- (filled symbols) vs. Br^- (hollow symbols) solutions near room temperature for various commercial alloys as indicated in the top scale (Guo & Ives, 1990; Abd El Meguid, 1997; Ernst & Newman, 2008; Pahlavan et al., 2019a).

PRE_N (pitting resistance equivalent with nitrogen) number (ISO 2010):

$$PRE_N = wt.\%\,Cr + 3.3\,(wt.\%\,Mo + 0.5\,wt.\%\,W) + 16\,wt.\%\,N$$

In the literature, there are similar versions of this equation that do not consider the beneficial effect of W or with different factors for N (Malik et al., 1994, 1995; Sedriks, 1996; Szklarska-Smialowska, 2005). E_{pit} in seawater (Malik et al., 1994, 1995) and CPT in ferric chloride solutions (Sedriks, 1996) both increase with an increase in PRE_N. Similar correlations exist for crevice corrosion critical parameters (Sedriks, 1996). CPT increases with PRE_N in 35,500 ppm Br^- solutions, but the slope in the CPT vs. PRE_N graph was lower in Br^- than in Cl^- solutions (Ozturk & Grubb, 2012). Considering this finding, thumb or engineering rules valid in chloride solutions, like $PRE_N > 40$ for resistance to localized corrosion in seawater at room temperature (Norsok, 2014; Francis & Hebdon, 2015), will not be valid for bromide solutions of similar concentrations. The critical pitting temperature of austenitic UNS N08904 ($PRE_N = 34.9$) and UNS S31254 ($PRE_N = 43.5$) stainless steel is near room temperature in Br^- solutions (Guo & Ives, 1990; Abd El Meguid, 1997), i.e. more than 30°C lower than values measured in Cl^- solutions (Guo & Ives, 1990). Given those results, the use of high PRE_N (and in particular, high Mo) stainless steels for mitigation of pitting corrosion is less effective in Br^- than in Cl^- solutions.

6 Stress corrosion cracking in halides solutions

Austenitic stainless steels suffer SCC in the presence of Cl^- ions (Scully, 1968; Hänninen, 1979; Cragnolino & Macdonald, 1982; Sedriks, 1996; Streicher, 2011), both in the fully solubilized and sensitized microstructures. The crack path in Cl^- solutions can be either transgranular (TG) or intergranular (IG), as reviewed by Cragnolino and Macdonald (1982). Similar to the situation for pitting corrosion, the SCC in halides other than Cl^- solutions received comparatively less attention. Some cases of SCC were reported for austenitic (Griess et al., 1985; Itzhak & Elias, 1994; Itzhak et al., 1996) and martensitic (Downs et al., 2007) stainless steels in the presence of bromides or other bromine species (Lee et al., 1983; Nordin, 1983). Similar to Cl^- solutions, sensitization is not required for SCC occurrence in Br^- solutions. Finally, a number of researchers conclude that I^- act as an inhibitor of Cl^- SCC of austenitic stainless steels (Overman, 1966; Uhlig & Cook, 1969; O'Dell & Brown, 1978; O'Dell et al., 1980; Pinkus et al., 1981; Itzhak & Eliezer, 1983).

While pitting corrosion was not observed in F^- solutions, sensitized stainless steels suffer IGSCC in this environment (Ward et al., 1969; Theus & Cels, 1974; Takemoto et al., 1985; Trabanelli et al., 1988; Zucchi et al., 1988; Shibata et al., 1993a,b; Whorlow et al., 1997), a problem that was researched mainly because the presence of F^- is common in thermal insulation materials (Whorlow & Hutto, 1997) and in fluxes used in welding processes (Ward et al., 1969; Takemoto et al., 1985). In contrast to Cl^- solutions, no instances of F^--induced SCC were reported up to date in fully solubilized microstructures, as will be discussed in depth below.

6.1 SCC testing techniques and apparent "thresholds" for SCC

A short discussion of different tests used to quantify the aggressiveness of the different halide anions toward the SCC of stainless steel is presented. It has first to be noticed that sensitized type 304 suffers IGSCC in slow strain rate tests (SSRT) even in oxygen-containing "pure water" at a temperature above 50°C (Ford & Povich, 1979; Ford & Silverman, 1980; Cragnolino & Macdonald, 1982; Congleton

& Sui, 1992). By "pure water," it is meant a solution with less than 5 ppb Cl^- (Congleton & Sui, 1992) or conductivity <0.3 μS/cm (Ford & Silverman, 1980). It was proposed that strain can expose bare metal to the environment, and if the potential is in a range where repassivation of grain boundaries is slower than the matrix, crack propagation can proceed even in the absence of aggressive ions (Ford & Povich, 1979; Ford & Silverman, 1980; Cragnolino & Macdonald, 1982). The presence of halide ions increases the SCC susceptibility, for example, the minimum oxygen concentration and the minimum potential for SCC occurrence in SSRT decrease with an increase in Cl^- concentration (Congleton & Sui, 1992).

Halide ions are typically required for cracking in constant deflection tests, like those depicted in Figure 3. Dana and Delong (1956) and Dana (1957) proposed in the 1950s the SCC test shown in Figure 3, left. The test mimics the leaching of chlorides in the insulation followed by concentration by evaporation at the stainless steel surface, simulating the environment in contact with a stainless steel pipe under thermal insulation. This test was standardized in 1971 in the ASTM C692 standard, and it is one of the alternatives listed in the current version of this standard (ASTM C692-13, 2018). This test, however, is limited to "wicking-type" thermal insulation. Those materials wet completely when partially immersed in water. In this test, chlorides and other ions leach in the deionized (DI) water and concentrate on the surface of a U-bend stainless steel specimen. Temperature is controlled by the Joule effect with a transformer, connected either to a resistance heater taped to the specimen, as originally proposed by Dana (1957) or directly to the specimen, as later standardized by ASTM C692 standard (Figure 3, left). The 304 stainless steel is sensitized by heating for 3 h at 649°C. This temperature is close to the nose of the time-temperature-sensitization curve of type 304 stainless steel (Sedriks, 1996). The specimen is then bent into a U shape and stressed to 30 ksi (207 MPa) with a bolt and nut, and placed in the testing apparatus depicted in Figure 3, left. An insulation specimen passes the test if there are no cracks in the stainless steel surface after a 28-day period. In an alternative method (Hutto et al., 1985; Whitaker et al., 1990), temperature is controlled with a steam-heated pipe, and the DI water is dripped over the insulating material with a peristaltic pump (Figure 3, right). This alternative method was incorporated to ASTM C692 in the 1990 edition, and it has the advantage that it is applicable to both wicking and non-wicking thermal insulators (Hutto et al., 1985), while also reproducing more closely the type of wetting of an insulator most likely to be encountered in "real life" service. Prior to using either of the tests depicted in Figure 3 for qualification of insulating materials, the standard (ASTM C692-13, 2018) requires that the test method and sensitized stainless steel must be tested with pure water (less than 0.1 ppm Cl^-) and with a 1500-ppm Cl^- solution. Four coupons must crack in the Cl^- solution, and none of the four coupons should crack in pure water. Notice that similar solution conditions than those of the "blank" test might produce cracking of a sensitized stainless steel tested in a SSRT. In other words, the observed or apparent threshold conditions for cracking are dependent on the test method used.

"Thresholds" for SCC, i.e. a threshold aggressive anion concentration, potential, temperature, and stress intensity factor, are supposedly critical parameters above which SCC is possible and below which immunity is granted. Threshold values are usually defined considering material performance in short-term laboratory tests, performed under aggressive conditions (Andresen, 2019). Immunity is associated with successful performance in an accelerated

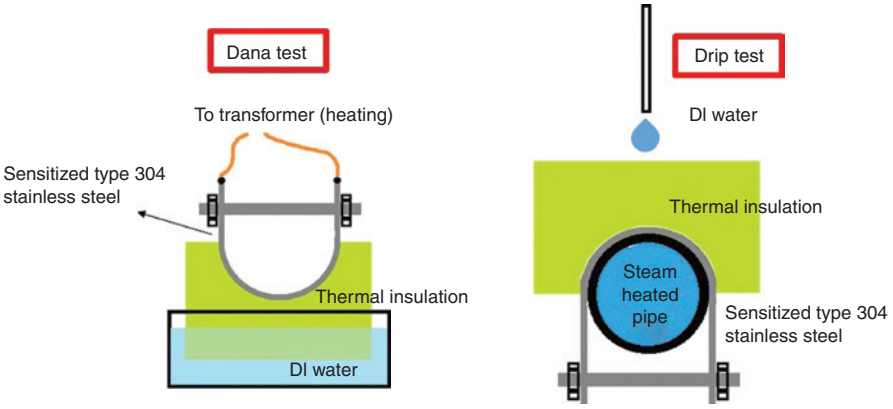

Figure 3: Alternative tests for laboratory studies of stress corrosion cracking under thermal insulation, after ASTM C692 (ASTM C692-13, 2018).

laboratory test, which often implies the absence of crack initiation after a certain time. For constant load and constant deflection tests, exposure time is often set to 30 days (Sridhar et al., 2017). After finishing the test, specimens are analyzed; however, there could be ambiguity in the minimum dimensions that a flaw or defect must have to be considered an initiated crack. In addition, it could be argued that cracks could have initiated if the exposure time was longer than the selected test duration.

It was proposed that rather than attempting to define thresholds for SCC, dependencies of crack growth rate with SCC variables should be characterized (Andresen, 2013, 2019). The SCC crack growth rate has a complex dependence on many variables, i.e. temperature, species in solution and their concentration, pH, stress, electrochemical potential, material microstructure, and strength (Staehle & Gorman, 2003). Careful experiments of *in situ* crack-growth rate measurements of stainless steels and nickel-based alloys in regions of supposed "immunity" to SCC in high-temperature water revealed in many instances crack propagation at a low growth rate (Andresen, 2019). It was proposed that a similar situation might be valid in other material-environment systems. If crack growth rate dependency with SCC variables and the actual defect size (or resolution of nondestructive testing methods) are known (Andresen & Ford, 1988), the residual life of the component or the optimum inspection interval can be assessed.

Much of the research conducted on the effect of F^-, I^-, and Br^- on SCC was based on accelerated tests, where the effect of one of those variables is explored while keeping the others constant. The identified region of "immunity" or crack growth at a low rate will not guarantee crack propagation at a low rate if one or more of the rest of the SCC variables or loading conditions are changed. Ideally, the dependency of crack growth rate with each of the variables that control SCC should be studied, but the equipment required is more sophisticated, and tests are more expensive.

6.2 SCC in sulfuric acid + halide ion solutions

Most cases of SCC occur when the bulk surface of the stainless steel is in the passive state. However, it has been shown (Acello & Greene, 1962; Asawa, 1971, 1987) that dilute additions of Cl^-, Br^-, and I^- to a H_2SO_4 solution cause the SCC of the solution annealed type 304 stainless steel. This occurs in a specific range of halide ion concentration and at a potential close to the corrosion potential, where the alloy is actively dissolving. Outside this potential range, the alloy failed by uniform attack or water-line corrosion (Asawa, 1987). Cl^-, Br^-, and I^- acted as dissolution inhibitors when their concentrations were below 10^{-1}, 2×10^{-3}, and 3×10^{-4} M, respectively; beyond these concentrations, they promoted uniform corrosion(Asawa, 1987). SCC was observed in a potential and halide ion concentration where the uniform dissolution rate was lower than 1 nm/s, regardless of the nature of the halide ion (Asawa, 1987).

6.3 Effect of halides other than Cl^- on SCC in high-temperature water

A few studies addressed the effect of halides other than Cl^- on high temperature (around 300°C) water, an environment relevant for cooling water of nuclear power plants. The SCC in high-temperature water of types 304 and 316 stainless steel in the presence of Br^- ions (Kumada, 1996) is characterized by a transgranular crack path, and the reported threshold amounts of Br^- and dissolved oxygen required for cracking in accelerated tests at 250°C were 50 ppm and 0.1 ppm, respectively. Fluorides at a concentration level of 1–10 ppm favored intergranular cracking in constant load tests of thermally sensitized type 304 and type 316 stainless steel in high-temperature water with 10 ppm O_2 (Berry et al., 1973). Finally, it was reported (Chung et al., 1996) that fluorides favor IGSCC of irradiated type 304 stainless steel, where Cr depletion at the grain boundary was caused by irradiation.

6.4 Critical potential for SCC in halide solutions

The rest of this review will mainly address SCC of stainless steels in halide solutions at lower temperatures and at bulk pH values where a passive film is stable, but might rupture locally giving localized corrosion phenomena like pitting or crevice corrosion. Under such conditions, Cl^- SCC initiates from localized attack in pits and crevices (Newman, 2001). It was proposed that a lower bound for the critical potential for Cl^- SCC of stainless steels and other corrosion-resistant alloys is the repassivation potential for localized corrosion, E_{rp} (Tsujikawa et al., 1994; Cragnolino et al., 1996; Sridhar et al., 2017). E_{rp} might correspond to the pitting or crevice repassivation potential, depending on the type of localized corrosion process that is occurring. Electrochemical techniques for measuring E_{rp} are described in the literature (Sridhar et al., 2017). Below this potential, any initiated crack or flaw in the passive film would be arrested by repassivation of the film

(Cragnolino et al., 1994). This condition of $E_{corr} > E_{rp}$ for SCC crack propagation is necessary, but not a sufficient condition. Notice that an excessively high potential would cause crack blunting by pitting or crevice corrosion (Tsujikawa et al., 1994; Newman, 2001). Crack velocity has to be larger than the rate of localized corrosion, and because an increase in temperature causes a higher increase in crack velocity due to a larger activation energy (Che-Sheng Chen et al., 1997; Newman, 2001), this results in a critical temperature for SCC (Che-Sheng Chen et al., 1997). Finally, plastic strain rate is required at the crack tip, for a local disruption of the passive film (Andresen & Ford, 1988; Sridhar et al., 2017; Andresen, 2019).

Extensive testing by Tsujikawa et al. (1994), using spot-welded specimens of various austenitic stainless steels exposed to Cl^- solutions confirmed that initiation of cracks required a potential greater than E_{rp}. In those tests, a small sheet of stainless steel was spot-welded on top of a larger coupon, generating both a crevice and weld nuggets with residual stresses around them. The SSRT of Fe-Ni-Cr-Mo alloys 316L and 825 in Cl^- solutions confirmed that at potentials below E_{rp}, specimens failed in a ductile fashion (Cragnolino et al., 1996; Pan et al., 2000). For the same system, using pre-cracked wedge-loaded fracture mechanics specimens, crack growth was only detected when the potential was above E_{rp} (Pan et al., 2000), and no cracks were observed below E_{rp} in constant deflection tests (Cragnolino et al., 1996). Recently, *in situ* measurement of crack growth rate on pre-cracked specimens confirmed (Gui et al., 2014; Sridhar et al., 2017) a decrease in crack growth rate of almost two orders of magnitude as the potential decreased below E_{rp}, for a 13-Cr supermartensitic stainless steel in a 0.3 M NaCl solution at 85°C.

Summarizing, depending on the test method used, it is inferred that for stainless steels in Cl^- solutions at a potential below E_{rp}, SCC initiation or crack growth rate is extremely difficult or decreases abruptly, respectively. This dependence of SCC with potential, assuming a similar cracking mechanism in solutions of the other halides, is useful for interpreting SCC results reported for the rest of the halides. For stainless steels with no or little content of Mo, the E_{rp} (Tzaneva et al., 2006) in halide solutions increases in the same order as E_{pit}, i.e. $Cl^- < Br^- < I^-$. In this regard, chlorides are often reported (Scully, 1968; Davis, 1994; Whorlow et al., 1997) as the most effective of the halide ions to promote SCC of stainless steels. Likewise, considering the absence of stable localized corrosion of stainless steels in F^- solutions (Tzaneva et al., 2006; Macdonald & Lei, 2016; Pahlavan et al., 2016), SCC should not be expected in F^- solutions. As previously mentioned, fluoride SCC is exclusively observed in sensitized microstructures (Zucchi et al., 1988), probably because the chromium-depleted region near the grain boundary repassivates slower than the matrix in the presence of F^- ions.

6.5 IGSCC in F^- solutions

Sensitized stainless steels suffer IGSCC in the presence of F^- ions (Ward et al., 1969; Theus & Cels, 1974; Takemoto et al., 1985; Trabanelli et al., 1988; Zucchi et al., 1988; Shibata et al., 1993a,b), even in dilute 5×10^{-5} M (1 ppm) F^- solutions at room temperature, as determined by the SSRT (Trabanelli et al., 1988; Zucchi et al., 1988). IGSCC was also reported in constant load tests in 10^{-4} M (2 ppm) F^- solutions at room temperature (Trabanelli et al., 1988). By comparison of results available in the literature (Takemoto et al., 1985; Trabanelli et al., 1988; Zucchi et al., 1988), it is observed that IGSCC occurrence requires more aggressive conditions (higher T or higher F^- concentration) in constant load or constant deflection tests than in SSRT.

6.5.1 Effect of potential on F^- IGSCC

The breakdown of the passive layer was not observed in conventional polarization curves of sensitized stainless steel in F^- solutions (Zucchi et al., 1988), as previously discussed. In contrast, a breakdown potential (E_b) associated to intergranular cracking was observed when *stressed* specimens were anodically polarized in F^- solutions (Theus & Cels, 1974) at 65°C. According to the authors (Theus & Cels, 1974), IGSCC occurred when $E_{corr} > E_b$. E_b decreased with pH and with F^- concentration in the range of 1–1000 ppm. E_{corr} decreased with pH, but it was fairly independent of F^- concentration. Therefore, a decrease in pH or an increase in F^- concentration increased cracking susceptibility. Notice the difference of this cracking condition with $E_{corr} > E_{rp}$ for the SCC of stainless steel (Tsujikawa et al., 1994; Cragnolino et al., 1996; Sridhar et al., 2017). The E_b determined by Theus and Cels (1974) is a potentiodynamically determined potential for *initiation*, and it might vary with experimental parameters like crack incubation time and potential scanning rate. While specimens exhibited cracks when the potential was above E_b, some specimens exhibited cracking when polarized *below* E_b. A more conservative potential to prevent cracking might be the repassivation potential, E_{rp}, measured during a backward scan in the active direction after controlled localized corrosion propagation (Szklarska-Smialowska, 2005; Sridhar et al., 2017). Theus and Cels (1974) did not conduct cyclic potentiodynamic tests for E_{rp} determination, but the

existence of an arrest potential for intergranular attack in F^- solutions is hypothesized. The existence of a crack arrest or critical potential in F^- solutions can be inferred from tests conducted by Zucchi et al. (1988). The authors performed an SSRT of sensitized stainless steel wires and then after crack initiation; the deformation was kept constant. Crack propagation could be detected by monitoring the load as a function of time: crack propagation caused a decrease in load, and the load remained constant when the crack was arrested (Zucchi et al., 1988). It was verified that crack propagated and arrested as the potential was switched within or outside the crack propagation potential range, respectively. For example, for a 200-ppm F^- solution at 25°C, crack propagation occurred within −0.4 and +0.4 V_{SCE}. The upper potential limit might correspond to crack blunting, but this was not discussed in depth by the authors. Finally, the minimum crack propagation rate that can be resolved with this technique was not reported in the paper.

6.5.2 Effect of sensitization on F^- IGSCC

In contrast to Cl^- SCC, a solution annealing heat treatment completely prevents F^- IGSCC (Ward et al., 1969; Theus & Cels, 1974). Transgranular branching and pitting attack commonly observed in tests of Cl^- SCC of sensitized type 304 SS are not observed in F^- solutions (Ward et al., 1969). Those results suggest that F^- attack is restricted to the intergranular region. Theus and Cels (1974) argue that the dependence of IGSCC with parameters of the sensitizing thermal cycle is difficult to assess. This issue could be solved with a systematic study of the dependence of F^- IGSCC with the degree of sensitization (DOS). The thermal cycle affects DOS, which can be defined as the extent of Cr depletion near the grain boundary (Parvathavarthini & Mudali, 2014). DOS can be quantified by coverage (fraction of total grain boundary depleted in Cr), depth (minimum concentration of Cr), and width (distance from grain boundary with a depleted Cr content) (Parvathavarthini & Mudali, 2014). DOS can be estimated with electrochemical techniques, as recently reviewed by Parvathavarthini and Mudali (2014).

6.5.3 Effect of temperature and F^- concentration on F^- IGSCC

Similar to the case for Cl^- SCC (Speidel, 1981), an increase in temperature from 25°C to 80°C increases the kinetics of the attack, according to Zucchi et al. (1988) and Ward et al. (1969). Measurements of time to failure at constant load and the ductility loss in the SSRT suggest that the aggressiveness of F^- increases with its concentration in the solutions, from 10^{-5} to 10^{-2} M (0.2–200 ppm F^-) (Trabanelli et al., 1988; Zucchi et al. 1988). This is in accord with the decrease in breakdown potential in anodic polarization curves of stressed specimens reported by Theus and Cels (1974), from 5×10^{-5} to 5×10^{-2} M (1–1000 ppm F^-). Some authors claim that a maximum susceptibility to IGSCC occurs at an intermediate F^- concentration. Using SSRT, Shibata et al. (1993b) showed that the region of maximum susceptibility is around 450 ppm F^- (0.02 M). Likewise, Ward et al. (1969) reported that solutions with a concentration around 1 M F^- (20,000 ppm F^-) do not cause IGSCC. Adding Cl^- ions to a the F^- solution did not change the kinetics or mode of attack; hence, a synergism between those ions was discarded (Ward et al., 1969). Whorlow et al. (1997) drew similar conclusions, after adding F^- ions to a Cl^- solution. This solution had a Cl^- concentration just below the threshold amount required for SCC in constant deflection tests, as will be discussed in detail in the next section.

6.5.4 SCC of stainless steels under thermal insulation

SCC in F^- and $F^- + Cl^-$ solutions were mainly studied (Takemoto et al., 1985; Whorlow et al., 1997; Whorlow and Hutto, 1997) because those ions are common impurities found in materials for thermal insulation. This failure mechanism is also known as ESCC, where the "*E*" means that the water and halides involved in the cracking mechanism are *external* to the pipe, tank, or vessel. Pipes conveying high-temperature fluids are commonly wrapped with thermal insulation to minimize heat losses and to protect nearby personnel. Water from rain, nearby processes, or arising from steam condensation can wet the thermal insulation (Dana, 1957; Ahluwalia, 2006). Alternatively, vapor from the atmosphere can condensate on a surface that is temporarily below the dew point (Ahluwalia, 2006). Water lixiviates impurities in the thermal insulation, and upon contact with the hot stainless steel surface, those impurities are concentrated by evaporation of the solvent (Dana, 1957; Ahluwalia, 2006). If aggressive species, namely, $F^- + Cl^-$, are originally present in the thermal insulation material, this leaching and concentration process can create optimum environmental conditions for the SCC of the stainless steel. Most failures occur in equipment with the stainless steel surface at a temperature between 50°C and 175°C (Ahluwalia, 2006; NACE, 2017). Below this temperature, the concentration by evaporation is not significant, and the kinetics of SCC is low, and above 175°C, liquid water presence on the stainless steel surface is less frequent. More

conservatively (McIntyre, 1985), the upper temperature is listed as 260°C, the temperature below which some chloride salts retain their hydration water. However, even in equipment operating above the maximum temperature, it is necessary to consider possible SCC occurrence during start-up and shutdown (McIntyre, 1985).

The SCC of stainless steel under insulation, like any other SCC problem, requires tensile stresses on susceptible materials exposed to a given environment. Most stainless steel products contain sufficient residual stresses to cause SCC in an aggressive environment even without applied stresses (NACE, 2017). This situation worsens if welding or cold work is involved in the fabrication process. Decreasing stress can be impractical, and changing the material is economically infeasible, especially in operating plants. Therefore, most strategies for prevention of ESCC focus on the environment. Standard specifications, like ASTM C795 (ASTM C795-08, 2018), provide limits for the maximum concentration of Cl^- and F^- in thermal insulation in contact with stainless steel. Thermal insulation has to be qualified in a preproduction standard test (ASTM C692-13, 2018), Figure 3, where it is tested to determine if the amount of leachable Cl^-, F^-, and inhibitors in the thermal insulator can cause SCC in a sensitized type 304 stainless steel stressed specimen at high temperature. Once the chemical composition and production process of the insulator is thus qualified, standard test method ASTM C871 (ASTM C871-182018) is used to measure the chemical composition, specifically the concentration of chlorides, fluorides, sodium, and silicates of subsequent production lots. The maximum acceptable concentrations of Cl^- and F^- in the insulator are indicated in standard ASTM C795 (ASTM C795-08, 2018), as a function of the concentration of inhibiting species (sodium and silicates). Regulatory guide US NRC 1.36 (US Nuclear Regulatory Commission 2015), applicable to thermal insulation to be used in nuclear power plants, contains similar guidelines as those of ASTM C795. The historical evolution of those standards is briefly discussed below, and it is of interest because it shows changes in perception on the aggressiveness of F^-.

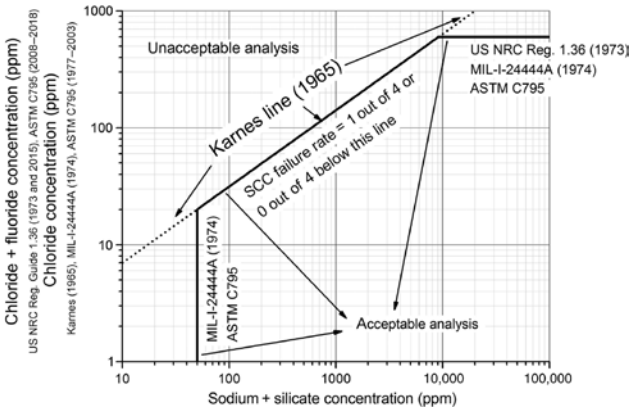

Figure 4: Acceptability curve of thermal insulation material, based on analysis of leachable halides (Cl^- or $Cl^- + F^-$, depending on the standard or specification as indicated) and leachable inhibitors (sodium + silicate). The diagonal line was first proposed by Karnes (Whitaker et al., 1990), and below this line, one out of four or zero out of four stainless steel specimens failed in an accelerated SCC test. Karnes line was adopted by subsequent standards and specifications, with major modifications as indicated.

6.5.5 Historical evolution of standards related to SCC of stainless steels under thermal insulation

Karnes in the 1960s determined that SCC can be inhibited if a certain amount of sodium and silicates are present in the thermal insulation material (Whitaker et al., 1990), and the results were reported in a Cl^- vs. Na^+ + silicates graph, known as the acceptability curve (Figure 4). In this graph, an arbitrary line separates the compositions of the insulator that cause the SCC in the stainless steel from those that do not. The line was traced considering that if no more than one out of four specimens failed, the test was considered a "pass" (Whitaker et al., 1990). While Karnes originally published the acceptability curve with Cl^- in the ordinate, the United States Atomic Energy Commission (USAEC) published the Regulatory Guide (RG) 1.36 in 1973 (US Atomic Energy Commission, 1973), where the ordinate was changed to $Cl^- + F^-$. Accordingly, the maximum $Cl^- + F^-$ content in the insulator was limited to 600 ppm. According to Whitaker et al. (1990), F^- was added to this regulatory guide because of the "chemical similarity and normally greater chemical aggressiveness of the fluoride," rather than based on experimentally measured effects of F^- on SCC. The United States military standard MIL-I-24244 (MIL-I-24244A 1974) issued in 1974 did not contain the F^- requirement, but this was added in a subsequent revision, to be consistent with RG 1.36 (Whitaker et al., 1990). Furthermore, the minimum sodium + silicate content was fixed at 50 ppm. ASTM C795, first published in 1977, did not contain the fluoride requirement in the acceptability curve (Figure 4), until the 2008 version, where it was added to "be consistent with other standards" (ASTM C795-08, 2018).

The $F^- + Cl^-$ vs. Cl^- controversy in the ordinate of the Karnes acceptability graph was studied in depth by Whorlow and Hutto (1997), in a report prepared for the US Nuclear Regulatory Commission and later published by ASTM (Whorlow et al., 1997). The experimental setup was similar to the one depicted in Figure 3 (right), but instead

of dripping DI water to leach ions from the insulator block, different solutions were dripped directly over the type 304 sensitized stainless steel surface, at a fixed flow rate for 28 days. The authors (Whorlow & Hutto, 1997) provided a chart to convert the concentration of ions in the solution (in mg/l) to the equivalent concentration in the insulator (in mg/kg), considering that in a real qualification test, the same flow rate would drip over the insulator but with DI water. In the absence of inhibiting species like sodium and silicates, the authors concluded that F^- ions cause SCC when they are in a concentration above 20 mg/kg (20 ppm) in the insulator. This is equivalent (Whorlow & Hutto, 1997) to 0.8 ppm of F^- in solution, which is further concentrated at the stainless steel surface by water evaporation. Therefore, this susceptibility to SCC of type 304 sensitized stainless steel in F^- solutions is in accord to the results reported elsewhere (Ward et al., 1969; Theus & Cels, 1974; Zucchi et al., 1988) with different experimental setups.

In comparison to Cl^- ions, SCC in F^- can be inhibited with considerably lower amounts of sodium and silicates, as summarized in Figure 5 (Whorlow & Hutto, 1997). Furthermore, when F^- ions were added to a solution of Cl^-, sodium, and silicate originally below the Karnes acceptability curve, SCC was not observed, despite the total $Cl^- + F^-$ content of the solution was in the cracking region of the acceptability graph (Figure 6). A single exception was the test run at 1000 ppm sodium + silicate and 100 ppm $Cl^- + 35$ ppm F^-, marked with an arrow in Figure 6. Based on those results, the authors (Whorlow & Hutto, 1997) discarded a synergistic effect between Cl^- and F^-, in accord with research previously published by Ward et al. (1969).

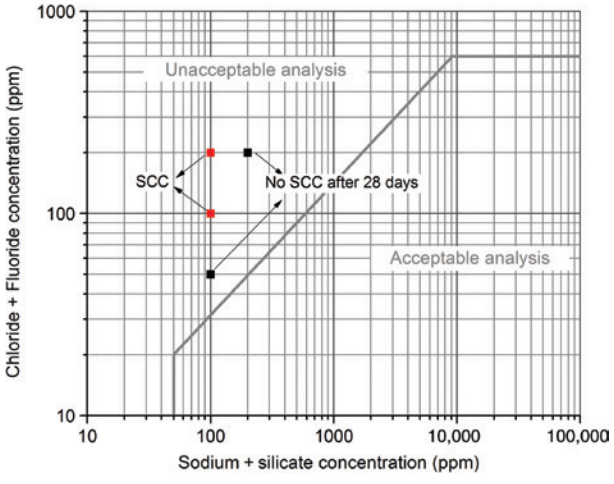

Figure 5: SCC of type 304 sensitized stainless steel in fluoride and sodium + silicate solutions; results are presented superimposed to ASTM C795 criteria for acceptability of thermal insulators (Whorlow & Hutto, 1997).

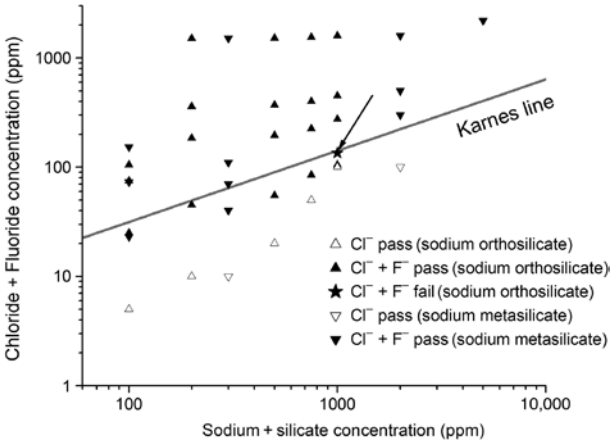

Figure 6: Effect of fluoride addition to a chloride, sodium, and silicate solution that passed the 28-day SCC tests. Karnes line given as reference. Except for the solution concentration marked with an arrow, no SCC was observed in $Cl^- + F^-$ solutions after 28 days. Adapted from Whorlow KM, Woolridge E0, and Hutto FB, Effect of halogens and inhibitors on the external stress corrosion cracking of type 304 austenitic stainless steel, Insulation materials: testing and applications: third volume, ASTM STP 1320, R.S. Graves and R.R. Zarr, Eds., copyright ASTM International, 100 Barr Harbor Drive, West Conshohocken PA19428, www.astm.org.

In other words, the amount of silicate and sodium required to inhibit Cl^- SCC seems to be sufficient to inhibit the effect of further additions of F^- (Whorlow & Hutto, 1997). Despite those results, when the US Nuclear Regulatory Commission (NRC) revised RG 1.36 in 2015 (US Nuclear Regulatory Commission, 2015), both Cl^- and F^- were considered as equally aggressive species and placed in the ordinate of Karnes acceptability graph. By this time, ASTM had already included F^- in the ordinate of Karnes graph, in the 2008 version of ASTM C795 (ASTM C795-08, 2018). The International Atomic Energy Agency (IAEA) published in 2011 the report "Stress corrosion cracking in light water reactors: good practices and lessons learned" (International Atomic Energy Agency, 2011), where the Karnes figure with $Cl^- + F^-$ in the ordinates was reproduced. In summary, current standards and regulatory guides on ESCC of austenitic stainless steels consider F^- as aggressive as Cl^-, despite contrary conclusions drawn in laboratory tests.

6.5.6 Some limitations of standards related to SCC of stainless steels under thermal insulation

Whorlow and coworkers (Whorlow & Hutto, 1997; Whorlow et al., 1997) reported that the inhibitor effectiveness was dependent on the type of silicate; the order of increasing effectiveness was sodium disilicate ($Na_2Si_2O_5$), sodium

metasilicate (Na_2SiO_3) and sodium orthosilicate (Na_4SiO_4). In other words, summarizing criticism on the acceptability curve of thermal insulation material (Figure 4), neither the aggressive ions plotted in ordinate or the inhibiting ions in the abscissa seem to be equally effective in promoting or preventing ESCC, respectively. Whorlow and coworkers reported the SCC of sensitized stainless steels in environments with chloride and sodium + silicate concentrations below the Karnes line, in other words, in the zone of acceptable analysis (Whorlow & Hutto 1997; Whorlow et al., 1997). The occurrence of SCC failures below the Karnes curve is not surprising because this curve was traced following the criterion that if none or one out of four SCC specimens failed for a given thermal insulator composition, the point was considered a pass (McIntyre, 1985; Whitaker et al., 1990). Current recommendations of ASTM C 795 require that the preproduction SCC test (ASTM C692-13, 2018) is passed if none of the specimens exhibit cracks. Lots produced with this validated production method and using similar ingredients are acceptable if their chemical composition falls inside the acceptable region (Figure 4) or if their chemical composition was validated with a pass in a preproduction SCC test. US REG 1.36 (US Nuclear Regulatory Commission, 2015) is more conservative because it not only requires that the chemical composition of the insulator falls in the acceptable region (Figure 4) but also that the chemical analysis of the $Cl^- + F^-$ content of the lot does not exceed 150% of the average values measured during preproduction qualification tests and that the sodium and silicate content is not below 50% of the average amount of those inhibitors measured during successful preproduction qualification tests.

Takemoto et al. (1985) questioned the 600 ppm high chloride limit in the acceptability graph (Figure 4). Using constant deflection tests with an initial stress above that required by ASTM C692 (ASTM C692-13, 2018), they proposed a threshold of 2000 ppm for a sensitized type 304 stainless steel and 3000 ppm for a solution annealed stainless steel, exposed to 95°C solutions. The difference in apparent Cl^- threshold concentration values could be explained considering its strong dependence with the rest of the testing variables.

In contrast to other studies (Ward et al., 1969; Whorlow & Hutto, 1997), Takemoto et al. (1985) suggest a synergistic effect of F^- and Cl^-, indicating that the 600 ppm high Cl^- limit can be much lower in the presence of F^-, decreasing to 200 ppm when the F^- concentration is 100 ppm. The authors state that F^- aggressiveness is maximum at 50°C, which is in conflict with results later published by Zucchi et al. (1988), where aggressiveness of F^- was higher at 80°C. Figure 7 summarizes the effect of F^- and Cl^- on

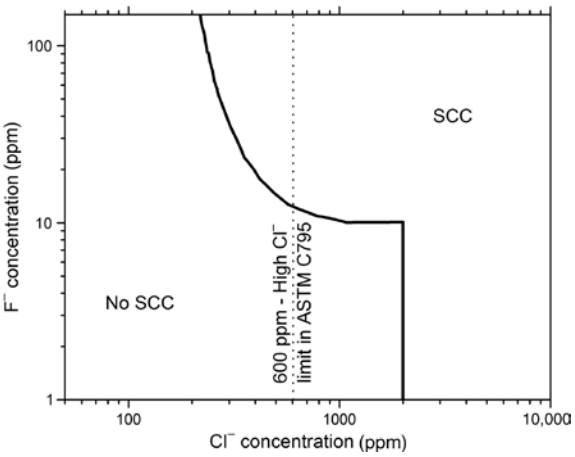

Figure 7: Summary of the effect of fluorides and chlorides on SCC at 50°C, for a solution without silicates and a type 304 sensitized stainless steel under constant deflection. Adapted from Takemoto et al. (1985). © NACE International, 1985.

the SCC of sensitized stainless steels at 50°C, according to Takemoto et al. (1985). The line that separates the SCC vs. No SCC zone was constructed based on laboratory tests in NaF and NaCl solutions without added silicates.

A major limitation of ASTM standards for ESCC management is that they only measure the capacity of inhibitors in the insulating material to guard against SCC failures caused by aggressive species in the insulating material. As reviewed by McIntyre (1985), Takemoto et al. (1985), and Hutto et al. (1985), and NACE International Standard SP0198-2017 (NACE, 2017), other potential sources of Cl^- of industrial relevance are the atmosphere, especially near coastal or industrial areas, or rainwater, processed, or potable water that might accidentally contact the thermal insulation. Insulation materials might have an excess of inhibitors to mitigate the effect of aggressive ions introduced from external sources. The ability of the insulation material to inhibit the effect of aggressive ions from outside sources can be tested using any of the experimental setups in Figure 3, if a Cl^- solution is used instead of DI water. In the "accelerated Dana test" a 1500-ppm (mg/l) Cl^- solution is used (Hutto et al., 1985; Whitaker et al., 1990), and an additional benefit is that the testing time is reduced from 28 to 6 days. However, it has not yet been included as an alternative procedure in ASTM C692. While inhibitors in the thermal insulator can offset the effect of externally introduced aggressive ions, it has to be noticed that if the equipment is severely wetted, the inhibitor might be leached and transported away from the surfaces needing inhibition (NACE, 2017).

If water reaches the stainless steel surface through cracks in the thermal insulator without soaking through

the insulation (McIntyre, 1985), the amount of leachable aggressive and inhibiting species in the insulator is not so relevant, and cracking can be controlled by the Cl^- or F^- concentration in the water. Guidelines for preventing water ingress to the thermal insulation are listed in the NACE International Standard SP0198-2017 (NACE, 2017). This standard addresses corrosion under insulation (CUI) under both stainless and carbon steels. Despite differences in their corrosion mechanisms, preventing water contact to the external surface of equipment is a common corrosion control strategy. An additional ESCC control strategy is the use of coatings or aluminum foil wrapping (Richardson & Fitzsimmons, 1985; NACE, 2017). The aluminum foil provides an additional barrier that prevents water and ions to be in contact with the stainless steel surface (Richardson & Fitzsimmons, 1985). More important, aluminum provides cathodic protection and decreases the corrosion potential of the stainless steel surface (Richardson & Fitzsimmons, 1985), which is effective for preventing Cl^- and F^- SCC (Smialowski & Rychcik, 1967; Rhodes, 1969; Uhlig & Cook, 1969; Theus & Cels, 1974).

Finally, it is noticed that the methodology of ESCC management with ASTM standards was developed based on results obtained with accelerated tests with smooth stainless steel coupons. However, if flaws or cracks are detected on a stainless steel component, it cannot be assured that they will not propagate during further use, even if new thermal insulation is installed, and its composition lays within the acceptability zone of Figure 4. Under such a scenario, knowledge of dependence of SCC growth rate with stress and environmental and material variables would be of much greater use for assessing the remaining life of the component (Andresen & Ford, 1988).

6.6 Br^- stress corrosion cracking

Pitting and crevice corrosion of stainless steels is observed in Br^- solutions, even in the fully solubilized condition. Therefore, considering a similar mechanism for SCC in Br^- vs. Cl^-, one of the necessary (Tsujikawa et al., 1994; Che-Sheng Chen et al., 1997; Newman, 2001; Sridhar et al., 2017) conditions for SCC would be fulfilled if $E_{Corr} > E_{rp}$. Br^- SCC was reported in environments of industrial interest, like completion fluids for the oil and gas industry (Downs et al., 2007; Sridhar et al., 2017) and brines for absorption refrigeration systems (Griess et al., 1985; Itzhak & Elias, 1994; Itzhak et al., 1996). With regard to laboratory tests, Rhodes (1969) reported SCC in 304 stainless steel exposed to 59% $MgBr_2$ solutions at 150°C, but cracking was not observed when the solution was more dilute than 36%. As a comparison, the SCC of 304 stainless steels occurs readily in accelerated laboratory tests in 20% $MgCl_2$ at 105°C (Brauns & Ternes, 1968), and more generally, at a temperature above 100°C, just a few ppm of Cl^- can cause SCC (Haruyama 1982) in industrial equipment. Therefore, albeit probably not as aggressive as Cl^-, the evidence reported suggests that concentrated, hot Br^- brines can cause SCC of stainless steels even in the fully solubilized condition.

Mo increases resistance to both localized corrosion and SCC of stainless steels in Cl^- solutions (Speidel, 1981; Sedriks, 1996; Prosek et al., 2009). This higher resistance is reflected in material selection guidelines; for example, to prevent Cl^- SCC in marine atmospheric environments, Norsok standard M-001 (Norsok 2014) sets the maximum operating temperature of type 6 Mo stainless steel in 120°C, higher than the 60°C set for a type 316 stainless steel (2.5 wt.% Mo). As illustrated in Figure 2, for alloys with a high concentration of Mo like stainless steel type 904L, Br^- can be more aggressive toward pitting than Cl^-. This higher aggressiveness of Br^- is also evidenced by a large decrease in CPT and CCT (Guo & Ives, 1990; Abd El Meguid, 1997; Ozturk & Grubb, 2012). An unsolved question is whether the higher aggressiveness of Br^- vs. Cl^- toward pitting and crevice corrosion in high Mo stainless steels implies also a higher SCC susceptibility in Br^- vs. Cl^- solutions.

6.6.1 SCC in Br^- containing completion fluids for oil and gas wells

Completion fluids used in high pressure, high-temperature oil, and gas wells might contain large concentrations of Br^-. When contaminated with O_2, or acid gases like CO_2 and H_2S, those brines can cause SCC in corrosion-resistant alloys like martensitic stainless steels (13 Cr-1Mo, 13 Cr-2Mo) (Downs et al., 2007). SCC was reported in laboratory studies of 13 Cr-2Mo stainless steel exposed to CO_2 and H_2S solutions at both 160°C and 40°C in concentrated Br^- solutions. Formate brines are often used in replacement of bromide brines to mitigate this problem (Downs et al., 2007; Sridhar et al., 2017).

6.6.2 SCC in Br^- brines for absorption refrigeration systems

LiBr commercial brines for use in absorption refrigeration systems can contain lithium chromates and lithium hydroxide (Griess et al., 1985; Igual Muñoz et al., 2003), added as corrosion inhibitors. These systems operate

under deaerated conditions, and besides the problem of integrity of materials, the release of hydrogen by the cathodic reaction at the corrosion potential produces non-condensable gases that decrease efficiency (Chandler, 1999). Desired corrosion rates in LiBr brines are below 1 mpy (25 μm/year). Various stainless steels and carbon steels in presence of chromates or other inhibitors fulfill this constraint (Chandler, 1999). The presence of chromates and deaerated conditions contribute to lower the corrosion potential (Igual Muñoz et al., 2003) and mitigate pitting corrosion. However, the high operating temperature (~150°C) might favor SCC.

With regard to SCC of stainless steels in LiBr brines, in a preliminary report, Griess et al. (1985) studied the SCC of austenitic type 304 stainless steel in 68% LiBr solutions at 160°C, conditions similar to those encountered in absorption refrigeration systems. The presence of oxygen was required for cracking of U-bend specimens, and none out of 20 specimens cracked under deaerated conditions (Griess et al., 1985). On the other hand, the SCC of types 304 and 316 stainless steels was reported by Itzhak et al. in 55% LiBr brines at 120°C and 140°C in deaerated conditions, both with the constant load (Itzhak & Elias, 1994) and slow strain rate technique (Itzhak et al., 1996). Specimens were studied in the "as-received" state (Itzhak & Elias, 1994; Itzhak et al., 1996), which included a 15% cold work estimated by comparison to fully annealed specimens of the same heat. The SCC crack path was generally transgranular, but depending on loading mode and temperature, mixed IG and TG cracks were observed for type 316 stainless steel. Itzhak et al. studied SCC in brines with pH varying from 6 to 11.6, and time to failure generally increased with increasing pH. The content of chlorides present as potential impurities in LiBr brines was not measured, and two different grades of LiBr salts were used by the authors, i.e. "analytical" (Itzhak & Elias, 1994) and "commercial" (Itzhak et al., 1996) grade.

Considering the concentration of LiBr solutions used in studies of evaluation of stainless steel for absorption refrigeration systems, it could be argued that trace amounts of chlorides in the salt could explain the SCC process. For example, Griess et al. (1985) reported that 37 ppm of chlorides were present in the brine as impurities from the LiBr salt, enough to cause chloride SCC at 160°C even in absence of Br^- (Sedriks, 1996). Despite this, the authors argue that Cl^- was not responsible for cracking because the Cl^- SCC inhibitors like chromate did not inhibit cracking in the concentrated LiBr salt (Griess et al., 1985). However, the role of chromate as a Cl^- SCC inhibitor is disputed (O'Dell & Brown, 1978) because despite stabilizing the passive film, it can raise the electrochemical potential. Stronger evidence to support the observation that cracking was actually due to Br^- is that according to U-bend constant deflection SCC tests conducted by Rhodes (1969), intentional additions of Cl^- to 36% $MgBr_2$ solutions did not induce cracking in type 304 stainless steel specimen, but SCC was observed in 59% $MgBr_2$ solutions at 150°C.

6.6.3 Br^- SCC under thermal insulation

The effect of Br^- on SCC of stainless steel under thermal insulation was not as deeply studied as the effect of F^- and Cl^-, probably because they are not as widely found in insulation as the lighter halides (Whorlow et al., 1997). The SCC of sensitized type 304 stainless steels in Br^- solutions was reported with an experimental setup similar to that shown in Figure 3 (right) (Whorlow et al., 1997). The presence of SCC cracks and pits was reported in sensitized type 304 stainless steel U-bend coupons heated to 100°C and exposed to 1500 ppm Br^- solutions (added as KBr), which was directly dripped over the stainless steel coupon. Under this experimental setup, the solution was concentrated by water evaporation at the hot stainless steel surface, so it is difficult to compare those experiments with those conducted in LiBr brines. The Br^- SCC of sensitized stainless steel could be inhibited with sodium orthosilicate, with a concentration of inhibitor that was much lower than required to inhibit Cl^- SCC (Whorlow & Hutto, 1997). Br^- ions were never included in ordinates of the acceptability curve of thermal insulation material (Figure 4). However, some analytical techniques (ASTM C871-18, 2018) to determine the Cl^- concentration in thermal insulation cannot discriminate between Cl^-, Br^-, and I^-, thus providing a false higher concentration of Cl^-. The concentration of inhibitor required in the thermal insulator would be increased accordingly, and considering that Cl^- is the most effective of those halides to cause ESCC in sensitized stainless steel, the possible effect of Br^- and I^- would be inhibited as well (Whorlow & Hutto, 1997).

6.6.4 SCC and localized corrosion in bromine compounds in desalination plants

The presence of Br^- ions in seawater can lead to corrosion issues in stainless steels used for multi-stage flash (MSF) desalination plants (Oldfield & Todd, 1981). Despite Cl^- being more concentrated in seawater than Br^-, Table 1, two different mechanisms (Oldfield & Todd, 1981; Lee et al., 1983) were proposed for the enrichment of bromine species in the vapor phase. Chlorine (Cl_2) is usually added

to feed-water as a biocide, and it can oxidize Br^- to Br_2, a reaction that is favored when pH is lower than 6 (Oldfield & Todd, 1981). Alternatively, bromamines can evolve from chlorinated seawater, if ammonia is present in seawater (Lee et al., 1983). Bromine and bromamines are then removed from the MSF plant together with non-condensable gases. Bromamines can decompose to hydrobromic acid and free bromine (Lee et al., 1983). Bromine is more oxidizing than oxygen (Lee et al., 1983), thus it raises the corrosion potential and favors pitting, crevice corrosion, and SCC. The SCC of type 316L stainless steel due to the presence of bromine species was reported in air ejector condenser systems (Black & Morris, 1981; Nordin, 1983) and venting pipes of MSF plants (Lee et al., 1983). Pitting and uniform corrosion of 316L were also reported in Br_2 solutions (Hodgkiess et al., 1985), and it was related to bromine reduction reaction, Eq. (1) that yields bromides. To prevent this type of failure, it was proposed to use higher alloyed stainless steel like 904L (Black & Morris, 1981; Nordin, 1983) or strict control of pH, chlorination level, and ammonia content in feedwater (Oldfield & Todd, 1981; Lee et al., 1983).

6.7 SCC in the presence of iodides and iodine

The SCC of zirconium alloys used for nuclear power reactor fuel cladding in iodine, a byproduct of the uranium fission reaction, is a well-documented problem (Cox, 1972; Wood, 1972; Sidky, 1998). While zirconium alloys are widely used as cladding in water-cooled reactors operating at temperatures close to 300°C, studies (Lobb & Jones, 1976; Lobb & Nicholson 1976; Lobb, 1978; Kiselevskii et al., 1993) conducted at 650°C and 750°C report that iodine vapor decreases creep resistance of austenitic stainless steels, a problem relevant for fuel cladding integrity of fast and advanced cooled reactors. Likewise, I_2 and I^- can be generated in aqueous homogeneous reactors, where uranium salts are dissolved in an aqueous solution that serves as moderator and coolant (Lillard, 2010). As reviewed by Lillard (2010), pitting and SCC of stainless steel in iodine species can affect the integrity of the off-gas extraction system of those reactors, required to remove the gases produced by radiolysis.

E_{pit} and E_{rp} of stainless steels in I^- solutions are larger than in Br^- or Cl^- solutions (Rhodes, 1969; Tzaneva et al., 2006; Macdonald & Lei, 2016). Therefore, the $E_{Corr} > E_{rp}$ (Tsujikawa et al., 1994; Che-Sheng Chen et al., 1997; Sridhar et al., 2017) criterion predicts SCC resistance in a wider range of potential in I^- vs. the rest of the halide solutions. Furthermore, under open-circuit conditions, the requirement that $E_{Corr} > E_{rp}$ (Tsujikawa et al., 1994; Che-Sheng Chen et al., 1997; Sridhar et al., 2017) is usually fulfilled by the presence of oxygen in the solution. However, iodide solutions are unstable in the presence of oxygen, reacting with it to give iodates or iodine (Eqs. (2) and (11)) (Pinkus et al., 1981; Itzhak & Eliezer, 1983):

$$2I^- + \frac{1}{2}O_2 + 2H^+ \rightarrow I_2 + H_2O \tag{11}$$

Given those considerations, in the case of I^- solutions, the reactants required for halide stress cracking might not be present simultaneously under common open-circuit conditions.

Nevertheless, SCC was observed in *sensitized* type 304 stainless steel. Whorlow and Hutto (1997), using an experimental setup similar to the one in Figure 3 (right), reported SCC in I^- solutions, added as KI. However, cracks were much shorter than those observed in chlorides, and cracking could be inhibited with silicates. In a previous attempt, SCC was not observed in iodide solutions (Whitaker et al., 1990), but this was explained based on a possible low carbon content of the stainless steel used. Current recommendations of ASTM C692 (ASTM C692-13, 2018) for evaluation of thermal insulation require a solution annealed type 304 stainless steel with carbon content in the range of 0.05–0.06%, which is then sensitized for 3 h at 649°C.

6.8 Inhibition of Cl^- SCC by I^- and I_2

Some researchers propose that iodide and iodine can act as inhibitors of SCC in Cl^- and Br^- solutions. Slow strain rate test (SSRT) studies (Huang et al., 1993) of solution annealed Ti-stabilized 321 stainless steel (UNS S32100) concluded that I^- and I_2 inhibit SCC of stainless steels in 0.5 M NaCl + 0.5 M HCl solutions at 55°C, with I^- being more effective than I_2. The fracture surface in the presence of 5 mmol/l KI was ductile with the presence of dimples. Similarly (Uhlig & Cook, 1969), additions of NaI to the boiling $MgCl_2$ SCC test solution increased the time to failure of solution annealed and cold-worked specimens of 304 stainless steel under constant load conditions, and no cracks were observed after 200 h of testing when more than 3.7% of NaI were added to the $MgCl_2$ solution. According to Itzhak et al. (Pinkus et al., 1981; Itzhak & Eliezer 1983), I^- acts as a cathodic inhibitor of chloride SCC, reacting with oxygen and protons according to Eq. (11). Evidence for the occurrence of this reaction was that the solution turned to yellow-brown color.

The corrosion potential in boiling 38% $MgCl_2$ + 15% NaI was 200 mV lower than the corrosion potential in boiling 38% $MgCl_2$ (Pinkus et al., 1981). A decrease in corrosion potential should contribute to inhibition of chloride SCC in boiling $MgCl_2$ solutions (Smialowski & Rychcik, 1967; Rhodes, 1969; Uhlig & Cook, 1969). Additions of 1% KI to a 55% LiBr brine of pH = 4 also inhibited Br^- SCC of type 316 stainless steel (Itzhak et al., 1996). Finally, some constant deflection tests performed on type 304 stainless steel with a setup similar to that shown in Figure 3 (right) (Whorlow et al., 1997) suggest that I^- is an ineffective inhibitor of Br^- and F^- SCC when the stainless steel is sensitized.

7 Summary and conclusions

Pitting and SCC of stainless steels is possible in halides other than chlorides. Several examples where this problem manifested in the industry were presented. Chloride is not only the halide most commonly encountered in environments of industrial relevance but also in most conditions the most aggressive. There is general agreement that the localized corrosion initiation (E_{pit}) and repassivation potential (E_{rp}) of stainless steels increase in the following order, $Cl^- < Br^- < I^-$. The intensity of SCC in halide solutions decreases in the same order, which can be understood considering that a necessary condition for SCC is that $E_{Corr} > E_{rp}$. A notable exception is that pitting in Br^- solutions can be more aggressive than in Cl^- solutions, for alloys with a high content of molybdenum. However, it is yet unsolved if high molybdenum stainless steels are more susceptible to SCC in Br^- than in Cl^- solutions. Detailed knowledge of the effect of alloying elements on Br^- localized corrosion and SCC would allow more rationality in the selection of stainless steels for bromide service.

For solubilized stainless steels, SCC was not observed in F^- and I^- solutions. For F^- solutions, this could be related to the pitting and localized corrosion immunity in those solutions. However, a sensitizing heat treatment decreases chromium content at the grain boundary, favoring localized rupture, and intergranular SCC is possible in the presence of stress. Passivity breakdown of stainless steels in iodide solutions would require excessively high potentials, and furthermore, iodides are unstable in the presence of dissolved oxygen, reacting with it to yield iodates and iodine. Hence, several researchers propose that iodides act as inhibitors for SCC of stainless steels in bromides and chlorides.

Acknowledgments: The author thanks Dr. Martín Rodríguez for helpful comments on the manuscript.

References

Abd El Meguid EA. Pitting corrosion behavior of type 904L stainless steel in sodium bromide solutions. Corrosion 1997; 53: 623–630.

Abd El Rehim SS, Abd El Wahaab SM, Abdel Maguid EA. Electrochemical behaviour of nickel anode in H_2SO_4 solutions and the effect of halide ions. Mater Corros 1986; 37: 550–555.

Acello SJ, Greene ND. Anodic protection of austenitic stainless steels in sulfuric acid-chloride media. Corrosion 1962; 18: 286t–290t.

Ahluwalia HS. Corrosion under insulation. In: Cramer SD, Covino BS, editors. ASM handbook Vol. 13C: corrosion: environments and industries. Materials Park, OH: ASM International, 2006: 654–658.

Andresen PL. Stress corrosion cracking of current structural materials in commercial nuclear power plants. Corrosion 2013; 69: 1024–1038.

Andresen PL. A brief history of environmental cracking in hot water. Corrosion 2019; 75: 240–253.

Andresen PL, Ford PF. Life prediction by mechanistic modeling and system monitoring of environmental cracking of iron and nickel alloys in aqueous systems. Mater Sci Eng A 1988; A103: 167–184.

Asawa M. Stress corrosion cracking of 18-8 austenitic stainless steel in sulfuric acid. Tetsu-to-Hagane 1971; 57: 1340–1349.

Asawa M. Stress corrosion cracking regions on contour maps of dissolution rates for AISI 304 stainless steel in sulfuric acid solutions with chloride, bromide, or iodide. Corrosion 1987; 43: 198–203.

ASTM A380-17. Standard practice for cleaning, descaling, and passivation of stainless steel parts, equipment, and systems. West Conshohocken, PA: ASTM, 2017.

ASTM C692-13. Standard test method for evaluating the influence of thermal insulations on external stress corrosion cracking tendency of austenitic stainless steel. West Conshohocken, PA: ASTM, 2018.

ASTM C795-08. Standard specification for thermal insulation for use in contact with austenitic stainless steel. West Conshohocken, PA: ASTM, 2018.

ASTM C871-18. Standard test methods for chemical analysis of thermal insulation materials for leachable chloride, fluoride, silicate, and sodium ions. West Conshohocken, PA: ASTM, 2018.

Berry WE, White EL, Boyd WK. Stress corrosion cracking of sensitized stainless steel in oxygenated high temperature water. Corrosion 1973; 29: 451–469.

Black DW, Morris RM. Experience in commissioning large desalination plants in the middle east. Desalination 1981; 39: 229–239.

Bocher F, Huang R, Scully JR. Prediction of critical crevice potentials for Ni-Cr-Mo alloys in simulated crevice solutions as a function of molybdenum content. Corrosion 2010; 66: 055002-1–055002-15.

Brauns E, Ternes H. Untersuchungen Über Die Transkristalline Spannungsrißkorrosion Austenitischer Chrom-Nickel-Stähle in Heißen Chloridlösungen. Werkstoffe Korros 1968; 19: 1–19.

Brown BF. Stress corrosion cracking control measures (NBS Monograph 156). Washington, DC: National Bureau of Standards, 1977.

Carroll WM, Lynskey EE. A crevice-free electrode assembly for the determination of reproducible breakdown potentials for stainless steels in halide environments. Corros Sci 1994; 36: 1667–1678.

Chambers C, Holliday AK. Modern inorganic chemistry. London, U.K.: Butterworth & Co., 1975.

Chandler T. Absorption chiller corrosion protection-SBIR Phase I Final Report – DOE Grant DE-FG03-98ER82658, 1999.

Che-Sheng Chen P, Shinohara T, Tsujikawa S. Applicability of the competition concept in determining the stress corrosion cracking behavior of austenitic stainless steels in chloride solutions. Zairyo-to-Kankyo 1997; 46: 313–320.

Chung HM, Ruther WE, Sanecki JE, Hins A, Zaluzec NJ, Kassner TF. Irradiation-assisted stress corrosion cracking of austenitic stainless steels: recent progress and new approaches. J Nucl Mater 1996; 239: 61–79.

Congleton J, Sui G. The stress corrosion cracking of heavily sensitized type 316 stainless steel in water in the temperature range 50–100°C. Corros Sci 1992; 33: 1691–1717.

Cox B. Environmentally induced cracking of zirconium alloys. Corrosion 1972; 28: 207–217.

Cragnolino G, Macdonald DD. Intergranular stress corrosion cracking of austenitic stainless steel at temperatures below 100°C – a review. Corrosion 1982; 38: 406–424.

Cragnolino G, Lin LF, Szklarska-Smialowska Z. Stress corrosion cracking of sensitized type 304 stainless steel in sulfate and chloride solutions at 250°C and 100°C. Corrosion 1981; 37: 312–320.

Cragnolino GA, Dunn DS, Sridhar N. Environmental effects on stress corrosion cracking of type 316l stainless steel and alloy 825 as high-level nuclear waste container materials, Prepared for Nuclear Regulatory Commission, CNWRA 94-028. San Antonio, TX: Center for Nuclear Waste Regulatory Analyses, 1994.

Cragnolino G, Dunn DS, Sridhar N. Environmental factors in the stress corrosion cracking of type 316l stainless steel and alloy 825 in chloride solutions. Corrosion 1996; 52: 194–203.

Crouse PL. Fluorine: a key enabling element in the nuclear fuel cycle. J South Afr Inst Min Met 2015; 115: 931–935.

Dana AW. Stress-corrosion cracking of insulated austenitic stainless steel. ASTM Bull 1957; 225: 46–52.

Dana AW, Delong WB. Topic of the month – stress-corrosion cracking test. Corrosion 1956; 12: 19–20.

Davis JR. Stainless steels ASM specialty handbook. Materials Park, OH: ASM International, 1994.

de Castro MAC, Wilde BE. The corrosion and passivation of iron in the presence of halide ions in aqueous solution. Corros Sci 1979; 19: 923–936.

Domínguez-Aguilar MA, Newman RC. Detection of deleterious phases in duplex stainless steel by weak galvanostatic polarization in alkaline solution. Corros Sci 2006; 48: 2577–2591.

Downs JD, Harris M, Benton W, Howard SK, Billingham M. New insights into the potential for environmental cracking of corrosion resistant alloys in high-density formate and bromide well completion brines at high temperature. Corrosion/2007, Paper 07097. Houston, TX: NACE International, 2007.

Ernst P, Newman RC. The interaction between alloyed molybdenum and dissolved bromide in the pitting corrosion of stainless steels. Electrochem Solid-State Lett 2008; 11: C1–C4.

Evans GJ, Nugraha T. A study of the kinetics of I_2 deposition on stainless steel sampling lines. Nucl Technol 2002; 140: 315–327.

Ford FP, Povich MJ. The effect of oxygen temperature combinations on the stress corrosion susceptibility of sensitized type 304 stainless steel in high purity water. Corrosion 1979; 35: 569–574.

Ford FP, Silverman M. The prediction of stress corrosion cracking of sensitized 304 stainless steel in 0.01 M Na_2SO_4 at 97°C. Corrosion 1980; 36: 558–565.

Francis R, Hebdon S. The selection of stainless steels for seawater pumps. Corrosion/2015, Paper C2015-5446. Houston, TX: NACE International, 2015.

Frankel GS. Pitting corrosion of metals – a review of the critical factors. J Electrochem Soc 1998; 145: 2186–2198.

Frankel GS, Li T, Scully JR. Localized corrosion: passive film breakdown vs pit growth. J Electrochem Soc 2017; 164: 180–181.

Galvele JR. Transport processes and the mechanism of pitting of metals. J Electrochem Soc 1976; 123: 464–474.

Gaudet GT, Mo WT, Hatton TA, Tester JW, Tilly J, Isaacs HS, Newman RC. Mass transfer and electrochemical kinetic interactions in localized pitting corrosion. AIChe J 1986; 32: 949–958.

Greenwood NN, Earnshaw A. Chemistry of the elements, 2nd ed. Oxford, UK: Butterworth-Heinemann, 1997.

Griess JC, DeVan JH, Perez Blanco H. ORNL/TM-9646 Corrosion of materials in absorption heating and refrigeration fluids. Oak Ridge, TN: Oak Ridge National Laboratory, 1985.

Gui F, Cao L, Thodla R, Sridhar N. Localized corrosion and stress corrosion cracking of corrosion resistant alloys in H_2S containing environment. Corrosion/2014, Paper 4482. Houston, TX: NACE International, 2014.

Guiñon JL, Garcia-Anton J, Pérez-Herranz V, Lacoste G. Corrosion of carbon steels, stainless steels, and titanium in aqueous lithium bromide solution. Corrosion 1994; 50: 240–246.

Guo R, Ives MB. Pitting susceptibility of stainless steels in bromide solutions at elevated temperatures. Corrosion 1990; 46: 125–129.

Hänninen HE. Influence of metallurgical variables on environment-sensitive cracking of austenitic alloys. Int Met Rev 1979; 24: 85–136.

Harris DC. Quantitative chemical analysis, 7th ed. New York: Freeman and Company, 2007.

Haruyama S. Stress corrosion cracking by cooling water of stainless steel shell and tube heat exchangers. Mater Perform 1982; 21: 14–19.

Hodgkiess T, Ng NK, Argyropoulos P. The corrosion behaviour of a number of materials exposed to bromine-containing environments. Desalination 1985; 55: 229–246.

Horvath J, Uhlig HH. Critical Potentials for pitting corrosion of Ni, Cr-Ni, Cr-Fe, and related stainless steels. J Electrochem Soc 1968; 115: 791–795.

Huang YL, Cao CN, Lu M, Lin HC. Inhibition effects of I^- and I_2 on stress corrosion cracking of stainless steel in acidic chloride solutions. Corrosion 1993; 49: 644–649.

Hutto FB, Tissot RG, Whitaker TE. A new apparatus and test procedure for running ASTM C 692 stress corrosion cracking

tests. In: Pollock WI, Barnhart JM, editors. Corrosion of Metals Under Thermal Insulation, ASTM STP 880. Philadelphia, PA: American Society for Testing and Materials, 1985: 211–219.
IAEA-Nuclear Energy Series. Stress corrosion cracking in light water reactors: good practices and lessons learned. Vienna, Austria: International Atomic Energy Agency, 2011.
Igual Muñoz A, García Antón J, Guiñón JL, Pérez Herranz V. Corrosion behavior and galvanic coupling of stainless steels, titanium, and alloy 33 in lithium bromide solutions. Corrosion 2003; 59: 606–615.
ISO 21457:2010(E) International Standard. Petroleum, petrochemical and natural gas industries – materials selection and corrosion control for oil and gas production systems. Geneva, Switzerland: ISO, 2010.
Ito K. Determination of iodide in natural water by ion chromatography. Anal Chem 1988; 69: 3628–3632.
Itzhak D, Elias O. Behavior of type 304 and type 316 austenitic stainless steels in 55 % lithium bromide heavy brine environments. Corrosion 1994; 50: 131–137.
Itzhak D, Eliezer D. The stress corrosion cracking of welded austenitic stainless steels in $MgCl_2$ solutions in the presence of NaI additions. Corros Sci 1983; 23: 1285–1291.
Itzhak D, Elias O, Greenberg Y. Behavior of type 316 austenitic stainless steel under slow strain rate technique conditions in lithium bromide heavy brine environments. Corrosion 1996; 52: 72–78.
Janik-Czachor M. Effect of halide ions on the nucleation of corrosion pits in iron. Mater Corros 1979; 30: 255–257.
Jesionek M, Szklarska-Smialowska Z. The inhibition of the dissolution of iron in sulfuric acid by halide ions. Corros Sci 1983; 23: 183–187.
Kaneko M, Isaacs HS. Pitting of stainless steel in bromide, chloride and bromide/chloride solutions. Corros Sci 2000; 42: 67–78.
Kaneko M, Isaacs HS. Effects of molybdenum on the pitting of ferritic- and austenitic-stainless steels in bromide and chloride solutions. Corros Sci 2002; 44: 1825–1834.
Khalil W, Haupt S, Strehblow HH. The thinning of the passive layer of iron by halides. Werkstoffe Korros 1985; 36: 16–21.
Kiselevskii VN, Kovalev VV, Neklyudov IM, Ozhigov LS. Corrosion-cracking resistance of austenitic stainless steel under stress in an iodine medium. Strength Mater 1993; 25: 864–869.
Koch GH. Localized corrosion in halides other than chlorides. Mater Perform 1993; 32: 54–58.
Kolotyrkin JAM. Pitting corrosion of metals. Corrosion 1963; 19: 261t–268t.
Kumada M. Bromide stress corrosion cracking of stainless steels in high-temperature water. Zairyo-To-Kankyo 1996; 45: 284–291.
Ladwig KJ, Blythe GM. Flue-gas desulfurization products and other air emissions controls. In: Robl T, Oberlink A, Jones R, editors. Coal combustion products (CCP's) characteristics, utilization and beneficiation. Duxford, United Kingdom: Woodhead Publishing, 2017: 67–95.
Laycock NJ, Newman RC. Localised dissolution kinetics, salt films and pitting potentials. Corros Sci 1997; 39: 1771–1790.
Lee WSW, Oldfield OW, Todd B. Corrosion problems caused by bromine formation in additive dosed MSF desalination plants. Desalination 1983; 44: 209–221.
Li T, Scully JR, Frankel GS. Localized corrosion: passive film breakdown vs. pit growth stability: Part III. A unifying set of principal parameters and criteria for pit stabilization and salt film formation. J Electrochem Soc 2018; 165: 762–770.
Li T, Scully JR, Frankel GS. Localized corrosion: passive film breakdown vs. pit growth stability: Part V. Validation of a new framework for pit growth stability using one-dimensional artificial pit electrodes. J Electrochem Soc 2019; 166: C3341–C3354.
Lide DR, editor. CRC handbook of chemistry and physics. Boca Raton, FL: CRC Press, 2005.
Lillard RS. A review of corrosion issues related to uranyl nitrate base aqueous homogeneous reactors. Corros Eng Sci Technol 2010; 45: 194–203.
Liu Y, Xu LN, Zhu JY, Meng Y. Pitting corrosion of 13Cr steel in aerated brine completion fluids. Mater Corros 2014; 65: 1096–1102.
Lobb RC. The effect of iodine vapour on creep rupture properties of nitride 20% Cr/25% Ni/Nb/1.5 Ti stainless steel. J Nucl Mater 1978; 74: 212–220.
Lobb RC, Jones RB. The influence of iodine vapour on creep rupture properties Of20%Cr/25%Ni/Nb stabilised stainless steel. J Nucl Mater 1976; 59: 280–292.
Lobb RC, Nicholson RD. The effect of iodine vapour on the creep rupture properties of M316 stainless steel. Mater Sci Eng 1976; 22: 157–165.
Macdonald DD, Lei X. Theoretical interpretation of anion size effects in passivity. J Electrochem Soc 2016; 163: 738–744.
Malik AU, Siddiqi NA, Andijani IN. Corrosion behavior of some highly alloyed stainless steels in seawater. Desalination 1994; 97: 189–197.
Malik AU, Siddiqi NA, Ahmad S, Andijani IN. The effect of dominant alloy additions on the corrosion behavior of some conventional and high alloy stainless steels in seawater. Corros Sci 1995; 37: 1521–1535.
Mankowski J, Szklarska-Smialowska Z. Studies on accumulation of chloride ions in pits growing during anodic polarization. Corros Sci 1975; 15: 493–501.
Mccoubrey JC. The acid strength of the hydrogen halides. Trans Faraday Soc 1955; 51: 743–747.
McIntyre D. Factors affecting the stress corrosion cracking of austenitic stainless steels under thermal insulation. In: Pollock WI, Barnhart JM, editors. Corrosion of metals under thermal insulation, ASTM STP 880. Philadelphia, PA: American Society for Testing and Materials, 1985: 27–41.
MIL-I-24244A. Insulation materials, thermal, with special corrosion and chloride requirements. Military Specification, 1974.
NACE International SP0198. Standard practice control of corrosion under thermal insulation and fireproofing materials – a systems approach. Houston, TX: NACE International, 2017.
Newman RC. 2001 W.R. Whitney Award Lecture: understanding the corrosion of stainless steel. Corrosion 2001; 57: 1030–1041.
Nguyen VA, Carcea AG, Ghaznavi M, Newman RC. The effect of cation complexation on the predicted "B" value in Galvele's pit model. J Electrochem Soc 2019; 166: C3297–C3304.
Nordin S. Studies on stainless steels for service in desalination plants. Desalination 1983; 44: 255–263.
Norsok Standard M-001-Materials Selection. Standards Norway, Lysaker, Norway, 2014.
O'Dell CS, Brown BF. Control of stress corrosion cracking by inhibitors (a review of the literature). Washington, DC: Chemistry Department, The American University, 1978.

O'Dell CS, Brown BF, Foley RT. An exploratory study of inhibition of intergranular stress corrosion cracking in sensitized type 304 stainless steel. Corrosion 1980; 36: 183–200.
Ohtsu T, Miyazawa M. Materials selection and corrosion management in a process containing halides, Corrosion/2012, Paper C2012-0001352. Houston, TX: NACE International, 2012.
Oldfield JW, Todd B. Corrosion problems caused by bromine formation in MSF desalination plants. Desalination 1981; 38: 233–245.
Overman RF. Using radioactive tracers to study chloride stress corrosion cracking of stainless steels. Corrosion 1966; 22: 48–52.
Ozturk B, Grubb JF. Corrosion of stainless steels and titanium in bromide-containing solutions. Corrosion/2012, Paper C2012-0001253. Houston, TX: NACE International, 2012.
Pahlavan S, Moazen S, Taji I, Saffar K, Hamrah M, Moayed MH, Mollazadeh Beidokhti S. Pitting Corrosion of martensitic stainless steel in halide bearing solutions. Corros Sci 2016; 112: 233–240.
Pahlavan S, Moayed MH, Mirjalili M. The contrast between the pitting corrosion of 316 SS in NaCl and NaBr solutions: Part I. Evolution of metastable pitting and stable pitting. J Electrochem Soc 2019a; 166: C65–C75.
Pahlavan S, Moayed MH, Mirjalili M. The contrast between the pitting corrosion of 316 SS in NaCl and NaBr solutions: Part II. Morphology, chemistry, and stabilization of the pits. J Electrochem Soc 2019b; 166: C321–C331.
Pan YM, Dunn DS, Cragnolino GA. Effects of environmental factors and potential on stress corrosion cracking of Fe-Ni-Cr-Mo Alloys in chloride solutions. In: Kane RD, editor. Environmentally assisted cracking: predictive methods for risk assessment and evaluation of materials, equipment, and structures, ASTM STP 1401. West Conshohocken, PA: American Society for Testing and Materials, 2000: 273–288.
Parvathavarthini N, Mudali UK. Electrochemical techniques for estimating the degree of sensitization in austenitic stainless steels. Corros Rev 2014; 32: 183–225.
Pinkus P, Eliezer D, Itzhak D. The influence of alkali-halide additions on the stress corrosion cracking of an austenitic stainless steel in $MgCl_2$ solution. Corros Sci 1981; 21: 417–423.
Pistorius PC, Burstein GT. Metastable pitting corrosion of stainless steel and the transition to stability. Philos. Trans. R. Soc. A Math. Phys. Eng. Sci. 1992; 341: 531–559.
Pourbaix M. Atlas of electrochemical equilibria in aqueous solutions. New York: Pergamon Press, 1966.
Prosek T, Iversen A, Taxén C, Thierry D. Low-temperature stress corrosion cracking of stainless steels in the atmosphere in the presence of chloride deposits. Corrosion 2009; 65: 105–117.
Rao P. Microstructural and microchemical studies in weld sensitized austenitic stainless steels. In: Abrams H, Maniar GN, Nail DA, Solomon HD, editors. MiCon 78: optimization of processing, properties, and service performance through microstructural control, ASTM STP 672. Philadelphia, PA: American Society for Testing and Materials, 1979: 321–333.
Rhodes PR. Mechanism of chloride stress corrosion cracking of austenitic stainless steels. Corrosion 1969; 25: 462–472.
Richardson JA, Fitzsimmons T. 1985. Use of aluminum foil for prevention of stress corrosion cracking of austenitic stainless steel under thermal insulation. In: Pollock WI, Barnhart JM, editors. Corrosion of metals under thermal insulation, ASTM STP 880. Philadelphia, PA: American Society for Testing and Materials, 1985: 188–198.
Scully JC. The electrochemical parameters of stress-corrosion cracking. Corros Sci 1968; 8: 513–523.
Sedriks AJ. Corrosion of stainless steels, 2nd ed. New York: John Wiley & Sons, 1996.
Sekine I, Usui H, Kitagawa S, Yuasa M, Silao L. The effect of fluoride ions on the corrosion of steel materials in H_2SO_4 and CH3COOH solutions. Corros Sci 1994; 36: 1411–1424.
Shibata T, Haruna T, Oki T. Initiation and growth of intergranular stress corrosion cracks for sensitized 304 stainless steel depending on NaF concentration of aqueous solution. Tetsu-to-Hagane 1993a; 79: 721–725.
Shibata T, Oki T, Haruna T. Stress corrosion cracking susceptibility of sensitized type 304 stainless steel in NaF solution evaluated by SSRT. Zairyo-to-Kankyo 1993b; 42: 15–19.
Sidky PS. Iodine stress corrosion cracking of zircaloy reactor cladding : iodine chemistry (a review). J Nucl Mater 1998; 256: 1–17.
Smialowski M, Rychcik M. Effect of potential and stress on time to failure of austenitic stainless steels in magnesium chloride solutions. Corrosion 1967; 23: 218–221.
Soltis J. passivity breakdown, pit initiation and propagation of pits in metallic materials – review. Corros Sci 2015; 90: 5–22.
Speidel MO. Stress Corrosion cracking of stainless steels in NaCI solutions. Metall Trans A 1981; 12A: 779–789.
Sridhar N, Thodla R, Gui F, Cao L, Anderko A. Corrosion-resistant alloy testing and selection for oil and gas production. Corros Eng Sci Technol 2017; 53: 75–89.
Srikhirin P, Aphornratana S, Chungpaibulpatana S. A review of absorption refrigeration technologies. Renew Sustain Energy Rev 2001; 5: 343–372.
Srinivasan J, Kelly RG. On a recent quantitative framework examining the critical factors for localized corrosion and its impact on the Galvele pit stability criterion. Corrosion 2017; 73: 613–633.
Staehle RW, Gorman JA. Quantitative assessment of submodes of stress corrosion cracking on the secondary side steam generator tubing in pressurized water reactors: Part 1. Corrosion 2003; 59: 931–994.
Stine CMA. Recovery of bromine from sea water. Ind Eng Chem 1929; 21: 434–442.
Streicher MA. Pitting corrosion of 18Cr–8Ni stainless steel. J Electrochem Soc 1956; 103: 375–390.
Streicher MA. Austenitic and ferritic stainless steels. In: Revie W, editor. Uhlig's corrosion handbook, 3rd ed. Hoboken, New Jersey: Wiley, 2011: 657–693.
Szklarska-Smialowska Z. Pitting and crevice corrosion. Houston, TX: NACE International, 2005.
Takemoto M, Shonohara T, Shirai M, Shinogaya T. External stress corrosion cracking (ESCC) of austenitic stainless steel. Mater Perform 1985; 24: 26–32.
Theus GJ, Cels JR. Fluoride induced intergranular stress corrosion cracking of sensitized stainless steel. In: Tedmon CS, editor. Corrosion problems in energy conversion and generation. Princeton, New Jersey: Corrosion Division, Electrochemical Society, 1974: 384–396.
Thomas VM, Bedford JA, Cicerone RJ. Bromine emissions from leaded gasoline. Geophys Res Lett 1997; 24: 1371–1374.
Thorvaldsson T, Salwén A. Measurement of diffusion coefficients for Cr at low temperatures in a type 304 stainless steel. Scr Metall 1984; 18: 739–742.

Tousek J. Eisenlochfrass in Alkalischen Halogenidlösungen. Corros Sci 1975; 15: 147–154.
Trabanelli G, Zucchi F, Demertzis G. Intergranular stress corrosion cracking of sensitized AISI 304 by fluoride ions and its inhibition. Key Eng Mater 1988; 20–28: 1905–1912.
Tsujikawa S, Shinohara T, Lichang W. Spot-welded specimen maintained above the crevice-repassivation potential to evaluate stress corrosion cracking susceptibility of stainless steels in NaCl solutions. In: Cragnolino G, Sridhar N, editors. Application of accelerated corrosion tests to service life prediction of materials, ASTM STP 1194. Philadelphia, PA: American Society for Testing and Materials, 1994: 340–354.
Tsukaue Y, Kudo A, Nakao G, Yamasaki H, Kimura S. Accumulation of trihalide ions caused by corrosion. Corrosion 1993; 49: 220–234.
Tsukaue Y, Nakao G, Takimoto Y, Yoshida K. Initiation behavior of pitting in stainless steels by accumulation of triiodide ions in water droplets. Corrosion 1994a; 50: 755–760.
Tsukaue Y, Yamasaki H, Nakao G. Characteristics of pit initiation of stainless steel in triiodide aqueous solution. Zairyo-to-Kankyo 1994b; 43: 487–492.
Tzaneva BR, Fachikov LB, Raicheff RG. Effect of halide anions and temperature on initiation of pitting in Cr–Mn–N and Cr–Ni steels. Corros Eng Sci Technol 2006; 41: 62–66.
Uhlig HH, Cook EW. Mechanism of inhibiting stress corrosion cracking of 18-8 stainless steel in $MgCl_2$ by acetates and nitrates. J Electrochem Soc 1969; 116: 173–177.
US Atomic Energy Commission-Regulatory Guide 1.36 – Nonmetallic Thermal Insulation for Austenitic Stainless Steel. Washington, DC: US Atomic Energy Commission – Directorate of Regulatory Standards, 1973.
US Nuclear Regulatory Commission – Regulatory Guide 1.36 – Nonmetallic Thermal Insulation for Austenitic Stainless Steel. Washington, DC: U.S. Nuclear Regulatory Commission – Office of Nuclear Regulatory Research, 2015.
Ward CT, Mathis DL, Staehle RW. Research in progress intergranular attack of sensitized austenitic stainless steel by water containing fluoride ions. Corrosion 1969; 25: 394–396.
Warner TB. Normal fluoride content of seawater. Deep-Sea Res 1971; 18: 1255–1263.
Whitaker TE, Whorlow KM, Hutto FB. New developments in test technology for ASTM C 692 (preproduction corrosion test for insulation to be used on austenitic stainless steel). In: McElroy DL, Kimpflen JF, editors. Insulation materials, testing, and applications, ASTM STP 1030. Philadelphia, PA: American Society for Testing and Materials, 1990: 688–698.
Whorlow KM, Hutto FB. NUREG/CR-6539 – effects of fluoride and other halogen ions on the external stress corrosion cracking of type 304 austenitic stainless steel. Washington, DC: U.S. Nuclear Regulatory Commission, 1997.
Whorlow KM, Woolridge EO, Hutto FB. Effect of halogens and inhibitors on the external stress corrosion cracking of type 304 austenitic stainless steel. In: Graves RS, Zarr RR, editors. Insulation materials: testing and applications: Third Volume, ASTM STP 1320. Philadelphia, PA: American Society for Testing and Materials, 1997: 485–497.
Willison MJ, Clarke AG, Zeki EM. Chloride aerosols in central Northern England. Atmos Environ 1989; 23: 2231–2239.
Wood JC. Factors affecting stress corrosion cracking of zircaloy in iodine vapour. J Nucl Mater 1972; 45: 105–122.
Wren JC, Glowa GA, Merritt J. Corrosion of stainless steel by gaseous I_2. J Nucl Mater 1999; 265: 161–177.
Yamamoto K, Hosoya K. Corrosivity of Br^- and Cl^- on duplex stainless steel. Mater Sci Eng A 1995; 198: 239–243.
Yamazaki O. Effect of fluoride ion on the pitting corrosion of type 304 stainless steel in neutral NaCl solution. Zairyo-to-Kankyo 1994; 43: 265–271.
Yamazaki O. Effect of fluoride ion on the crevice corrosion for type 304 stainless steel in neutral NaCl solution. Zairyo-to-Kankyo 1996; 45: 365–369.
Yamazaki O. Repassivation potential E_R for crevice corrosion of type 304 stainless steel/FPM-crevice in neutral NaCl/NaF solutions. Zairyo-To-Kankyo 1997; 46: 419–423.
Zucchi F, Trabanelli G, Demertzis G. The intergranular stress corrosion cracking of a sensitized AISI 304 in NaF and NaCl solutions. Corros Sci 1988; 28: 69–79.

Bionote

Mariano A. Kappes
Instituto Sabato (UNSAM/CNEA), CONICET, Comisión Nacional de Energía Atómica, Av. Gral. Paz 1499, San Martín, Buenos Aires 1650, Argentina. https://orcid.org/0000-0002-5708-5565
marianokappes@gmail.com

Mariano A. Kappes obtained his Bachelor's degree in Materials Science and Engineering at the Instituto Sabato in Argentina in 2006 and then obtained his PhD in 2011 at the Ohio State University. His PhD thesis was distinguished with the Morris Cohen Award, awarded annually by The Electrochemical Society to outstanding graduate research in the field of Corrosion. Since 2014, he is a research scientist at the National Agency of Atomic Energy in Argentina and a Professor at the National University of General San Martin. He holds a position at the National Scientific and Technical Research Council as scientist since 2015.